
A SURVEY OF DEEP LEARNING-BASED RADIOLOGY REPORT GENERATION USING MULTIMODAL DATA

Xinyi Wang, Graziela Figueredo, Ruizhe Li
The University of Nottingham
United Kingdom

Wei Emma Zhang, Weitong Chen
The University of Adelaide
Australia

Xin Chen *
The University of Nottingham
United Kingdom

ABSTRACT

Automatic radiology report generation can alleviate the workload for physicians and minimize regional disparities in medical resources, therefore becoming an important topic in the medical image analysis field. It is a challenging task, as the computational model needs to mimic physicians to obtain information from multi-modal input data (i.e., medical images, clinical information, medical knowledge, etc.), and produce comprehensive and accurate reports. Recently, numerous works emerged to address this issue using deep learning-based methods, such as transformers, contrastive learning, and knowledge-base construction. This survey summarizes the key techniques developed in the most recent works and proposes a general workflow for deep learning-based report generation with five main components, including multi-modality data acquisition, data preparation, feature learning, feature fusion/interaction, and report generation. The state-of-the-art methods for each of these components are highlighted. Additionally, training strategies, public datasets, evaluation methods, current challenges, and future directions in this field are summarized. We have also conducted a quantitative comparison between different methods under the same experimental setting. This is the most up-to-date survey that focuses on multi-modality inputs and data fusion for radiology report generation. The aim is to provide comprehensive and rich information for researchers interested in automatic clinical report generation and medical image analysis, especially when using multimodal inputs, and assist them in developing new algorithms to advance the field.

Keywords Report generation · Deep learning · Multimodal · Medical image analysis

1 Introduction

Medical images can offer detailed insights into bodies and help physicians screen, diagnose and monitor medical conditions without requiring invasive techniques [Beddiar et al., 2023, Liao et al., 2023]. Radiologists summarize the information extracted from medical imaging into radiological reports for clinical decision-making. The manual generation of reports is however labour-intensive, time-consuming, and requires extensive expertise [Beddiar et al., 2023]. Topol [2019] points out that the demand for medical image explanation greatly surpasses the current capacity of physicians in the United States. During an epidemic and with ageing populations, the situation can get worse. During the Covid-19 pandemic, for instance, in the UK, each radiologist was estimated to report as many as 100 images each day [Statistics, 2020]. This makes it challenging for radiologists to provide high-quality reports within the scheduled time. The current demand extends patient waiting time and increases the risk of disease transmission [Beddiar et al., 2023] and compromises patient care. The development of automatic report generation techniques can help alleviate this problem.

Automatic high-quality report generation is challenging. It is intrinsically a multi-modality problem [Tu et al., 2024, Yan et al., 2023]. In routine clinical practice, to produce clear, correct, concise, complete, consistent, and coherent reports, radiologists need to combine information from images with information from other modality data, such as clinical history and related clinical measures. Previously developed techniques mostly considered images as input, while for the past three years, multi-modality deep learning developed very rapidly. An increasing number of research papers endeavored to emulate physicians by leveraging multi-modal data for the generation of diagnostic reports, as shown in Figure 1.

Most of the previous surveys on this topic [Kaur et al., 2022, Beddiar et al., 2023, Liao et al., 2023, Shamshad et al., 2023, Liu et al., 2023a] did not include non-imaging inputs. Messina et al. [2022] considered non-imaging inputs, but only involved 6 papers. Totally, the previous surveys included 40 to 66 papers for report generation, primarily focusing on articles published before 2022. This survey differs from previous ones in three main contributions: (1) we analyse an additional 22 papers that utilize non-image inputs, and focuses

*Corresponding author: Xin Chen, xin.chen@nottingham.ac.uk

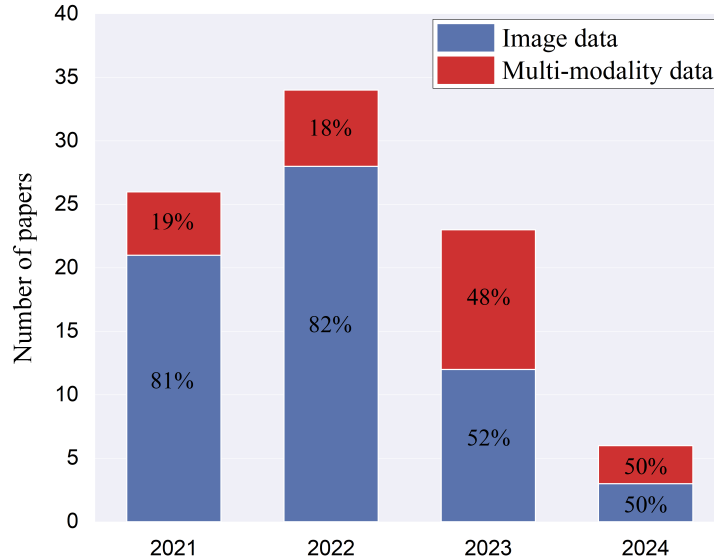


Figure 1: The distributions of reviewed papers using image data and multi-modality data as inputs per year from 2021 to 2024. The percentage denotes the input’s prevalence among articles published within the year.

on the acquisition, analysis, and integration of multi-modal inputs. To the best of our knowledge, it is the first review to investigate state-of-the-art multi-modal data processing techniques for report generation; (2) we examine 89 papers published from 2021 to 2024 to provide a comprehensive study on novel techniques in automatic report generation; and (3) we propose a general workflow for report generation with a taxonomy of approaches employed, and we summarize training strategies, public datasets, and mainstream evaluation methods, as shown in Figure 2. The workflow includes 5 key components: inputs, data preparation, feature learning, feature fusion, and report generation. Table A1 in Appendix A summarizes all works included in this survey.

The remainder of the paper is organized as follows. Section 2 introduces the paper search and selection process. Section 3 first provides a workflow of deep learning-based report generation, then analyses the techniques in each component of the workflow, and finally introduces the overall training strategies. Next, in sections 4 and 5, we introduce popular public datasets and evaluation methods, including metrics and expert evaluation. Section 6 compares the model performance of several papers under the same experimental setting. Lastly, we discuss challenges and perspectives on this topic in section 7 and provide a conclusion in section 8.

2 Search and selection of articles

Three search engines (Google Scholar, PubMed, and Springer) and four queries were employed to collect articles. They included “radiology report generation”, (medical OR medicine OR health OR radiology) AND (report OR description OR caption) AND generation, modal AND (medical OR medicine OR health OR radiology) AND (report OR description OR caption) AND generation, and “medical report generation”. Following the searches, the titles and abstracts of each article were read briefly to identify those that met the selection criteria. If there was uncertainty, the article was included to ensure relevant studies were not omitted. The selection criteria were framed around three aspects. First, we included articles published in the years 2021, 2022, 2023, and 2024 due to the significant number of developments using multi-modal technology in recent years. We aim to focus on the latest algorithms not covered in previous surveys. Second, the studies must be original researches focused on the automatic generation of full-text natural language radiology reports and include quantitative evaluation results. Techniques generating short captions of one or two sentences are excluded due to the differing nature of long report and sentence generation. Third, papers published in journals, conferences, and conference workshop proceedings were included. Moreover, papers uploaded on the arXiv website in 2023 and 2024 with over 30 citations were also selected. A total of 144 papers were identified using three search engines. In addition, by tracing the ancestry and descendants of papers, we identified another 24 papers. After removing duplicates, 97 publications were retained. We thoroughly read these works and applied exclusion criteria. First, at least one of the generated languages should be English. Second, at least one of the input data should be images. Finally, 89 works were included in the following analysis.

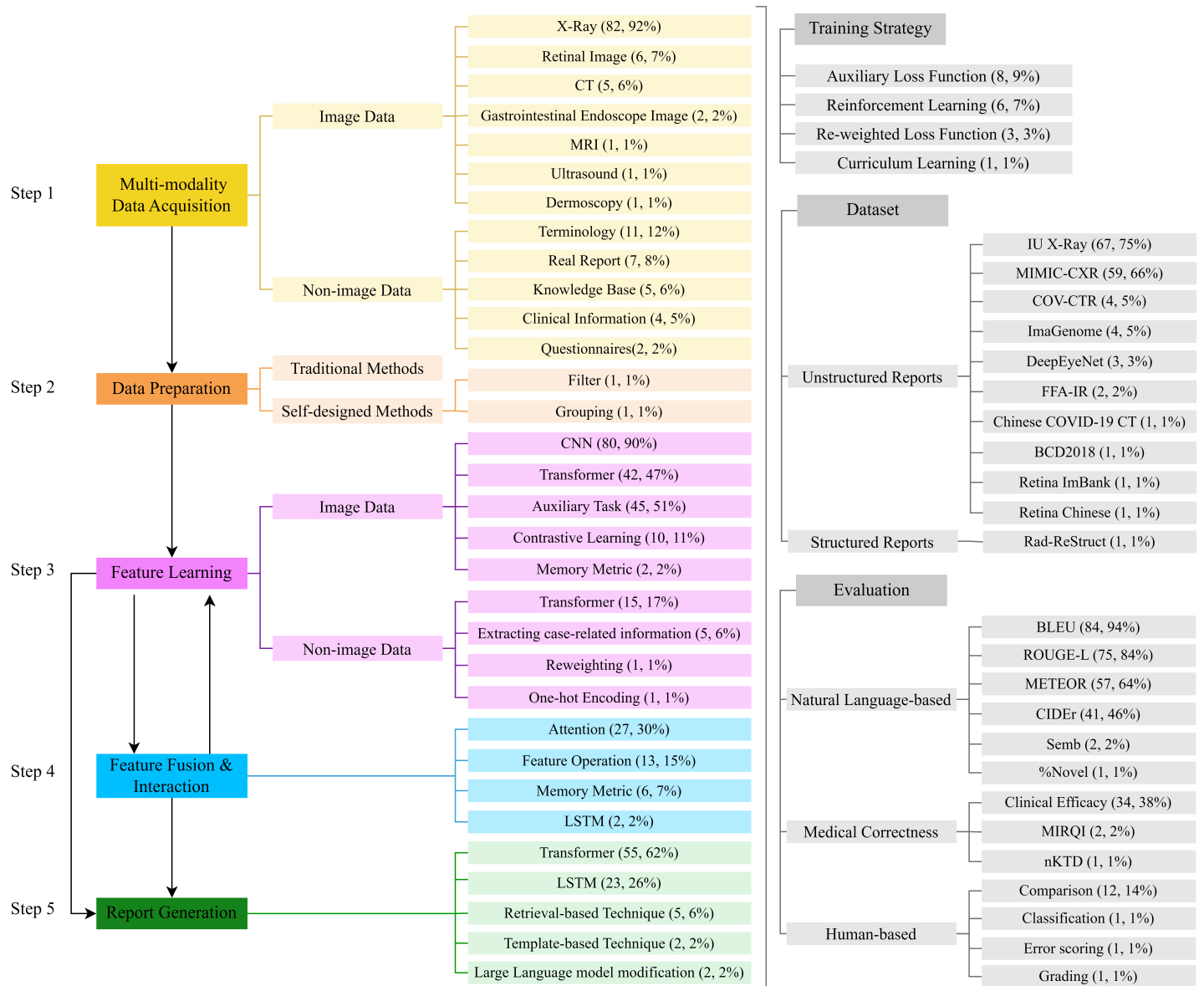


Figure 2: The summarized workflow of automatic radiology report generation. The fundamental components and key techniques are included. The (x, y%) for each method represents the number and percentage of papers used that technique in our survey.

3 Methods

Deep learning-based radiology report generation typically follows a standard workflow summarized in Figure 2. This section analyzes the techniques in the 89 works, based on the workflow identified. Overall, a basic radiology report generation framework consists of 5 steps: (1) multi-modality data acquisition (section 3.1); (2) data preparation (section 3.2); (3) feature learning (section 3.3); (4) feature fusion and interaction (section 3.4); and (5) report generation (Section 3.5). In addition, novel training strategies, including modifying loss functions, reinforcement learning, and curriculum learning, are described in Section 3.6.

Medical images, when analyzed with or without other types of data, are firstly prepared (step 2). Subsequently, they are input into feature extractors to perform feature learning (step 3), predominantly implemented using CNN or Transformer architectures, along with multiple enhancement modules (e.g., auxiliary task and contrastive learning). The feature extractors aim at extracting features relevant to report generation, and the enhancement modules are utilized to improve the expressiveness of the features. For certain approaches, a feature fusion and interaction module (step 4) is subsequently applied to align cross-modal data and mitigate the negative effects caused by differences between the visual and textual domains. After fusion and interaction, the features are conveyed back to the feature extractor or

directly input into the generator to generate the report (step 5). The training strategy is implemented to improve learning effectiveness during training. Table A1 in Appendix A presents detailed information for each paper across the five steps and training strategies.

3.1 Multimodality input data

The input data refers to the data received by the report generation system. During model training and inference, the data can vary; for example, both images and real reports are used as inputs during training, while only images are used during inference [Shetty et al., 2023]. However, the model learns from the distribution and features of the training data. If the testing data changes, mostly, the model will struggle to generalize, resulting in decreased performance. Therefore, in this section, we mainly introduce the acquisition of input data that is consistent between the training and testing phases in the reviewed papers. The input data includes:

- *Image data* includes X-ray, magnetic resonance imaging (MRI), computed tomography (CT), ultrasound, gastrointestinal endoscope image, retinal image, and dermoscopy image. Most papers we reviewed focus on generating medical reports for chest X-ray images (82 works). Other than chest diagnosis, retinal image is the second most prevalent image modality (6 works). The retinal image includes lots of categories, e.g., fundus fluorescein angiography and color fundus photography. Other works focus on chest CT (5 works), gastrointestinal endoscope image (2 works), spine MRI (1 work), dermoscopy image (1 work), and breast ultrasound images (1 work). Although some images are non-radiological, such as ophthalmic images, we still include their report-generation techniques in this survey.
- *Medical terminology* refers to medical terms and expressions, which are from keyword labels of images [Huang et al., 2021a,b, 2022, Liu et al., 2023b], or self-built corpora [Liu et al., 2021b, Cao et al., 2022, 2023, Xue et al., 2024, Gu et al., 2024, Li et al., 2023c], storing common descriptions found in medical reports.
- *Medical knowledge base* mostly records the connections between different organs and diseases, and is presented in a graph format. Graph is a fundamental data structure consisting of a set of nodes and edges, which can easily represent a set of subjects and their connections. The knowledge graph can primarily be obtained in two ways: 1) public datasets such as the RadGraph [Jain et al., 2021] used by two works [Yang et al., 2022, Li et al., 2023a]; 2) self-designed knowledge bases according to authoritative medical standards [Huang et al., 2023, Xu et al., 2023] or disease labels [Jia et al., 2022]. Yang et al. [2023] argued that manual graph construction is limited to diseases, further complicating the adaptation of these models for diverse datasets. To overcome it, they automatically constructed the medical knowledge based on real reports during training and leveraged the knowledge base during model inference.
- *Real texts report* is mostly obtained by data retrieval [Liu et al., 2021b, Song et al., 2022, Yang et al., 2022, Li et al., 2023a, Liu et al., 2023b, Li et al., 2023c, Jin et al., 2024]. For example, for each input image, Liu et al. [2021b] retrieved similar images from the training dataset and utilized the corresponding reports. This process mimics radiologists consulting previous medical case reports when drafting their own. In addition, Liu et al. [2023b] also obtained pre-defined sentences based on input terminologies.
- *Clinical information* encompasses patient demographics (e.g., age and gender), clinical observations, and medical histories. It is included within the indication section of radiology reports (see Figure 4).
- *Questionnaires*: report generation model can be trained in a visual question answering way [Tanwani et al., 2022, Pellegrini et al., 2023]. The questionnaires are provided by public datasets, such as VQA-Rad [Lau et al., 2018] and Rad-ReStruct [Pellegrini et al., 2023].

3.2 Data preparation

Data preparation endeavors to enhance data quality and prepare it for model deployment, typically encompassing data cleansing, transformation, and organization. Conventional preparation methods include image resizing and cropping, text tokenizing, converting all tokens to lowercase, removing non-alphabetic tokens, and implementing data augmentation procedures. The methods utilized in each paper are outlined in Table A1 in Appendix A, but it is worth noting that conventional preparation methods are so ubiquitous that some papers do not mention them. While the information is not recorded in the table, it does not mean the absence of a data preparation process.

Novel data preparation methods in the reviewed papers can be categorized into filtering [Ramesh et al., 2022] and grouping [Wang et al., 2022b]. Ramesh et al. [2022] argued that writing a radiology report necessitates referencing historical information, which inevitably included descriptors such as ‘again’ and ‘decrease’. However, these terms cannot be inferred from a single image, therefore Ramesh et al. filtered such descriptions in the reports. This exclusion was found to facilitate the model’s learning process.

Grouping refers to organizing sentences from ground truth reports into distinct sections, typically relying on keywords from pre-defined knowledge graphs and filtering rules. Each section describes a specific anatomical structure. Grouping aims to enable the generation system to process various types of sentences differently. For instance, Wang et al. [2022b] employed different decoders to generate descriptions for different anatomical structures. Alongside the reviewed papers, a recently released public dataset named ImaGenome [Wu et al., 2021] also includes grouping results in their annotation files (see Section 4). The grouping result becomes more easily accessible.

3.3 Feature learning

3.3.1 Image-based feature learning

Previous research primarily utilized CNNs as architectures for extracting image features, however, recently, an increasing number of researchers have opted for the use of Transformers due to their improved performance. Simultaneously, numerous studies proposed novel modules to enhance the model capability. In this section, the model architecture is first introduced, and subsequently enhancement modules are described. These modules include auxiliary tasks, contrastive learning, and memory metrics. The architecture and modules utilized in each paper are outlined in Table A1 in Appendix A.

CNN and Transformer encoder for feature extraction The statistics of the architectures used as image feature extractor are shown in Figure 3. In total, forty-six studies extract image features purely based on CNN models. Thirty-four works firstly encode images by CNN and then utilizes the Transformer layers to modify the embeddings. Eight works utilize a pure Transformer architecture to extract image features. Figure 3 shows a clear trend of more studies adopting CNN augmented with Transformer for image feature extraction.

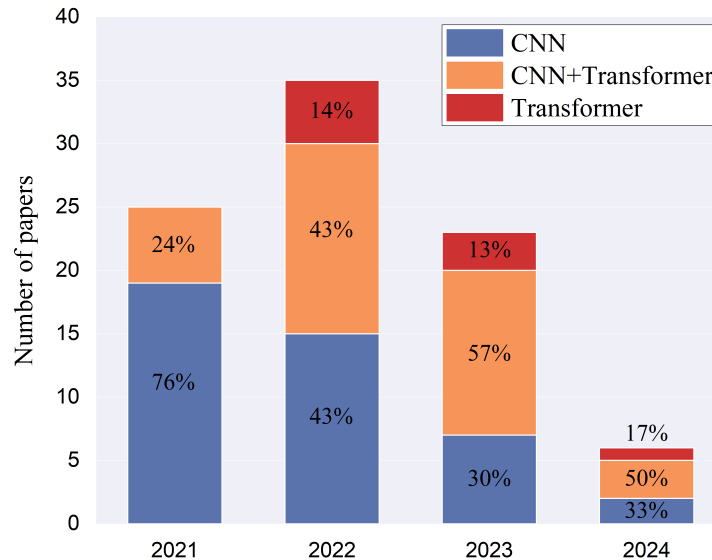


Figure 3: The statistics of the reviewed papers using different architectures to extract image features per year from 2021 to 2024. The percentage denotes the method’s prevalence among articles published within the year.

For CNN architecture, two works self-designed CNN models, while the other works built it based on different classical visual models, such as ResNet [He et al., 2016] (42 papers), DenseNet [Huang et al., 2017] (22 papers), VGG [Simonyan and Zisserman, 2014] (5 papers), Faster-RCNN [Ren et al., 2015] (5 papers), Inception-V3 [Szegedy et al., 2016] (1 paper), ResNeXt [Xie et al., 2017] (1 paper), EfficientNet [Tan and Le, 2019] (1 paper), and the Two-Stream Inflated 3D ConvNets (I3D) [Carreira and Zisserman, 2017] (1 paper). Pahwa et al. [2021] modified the HRNet [Sun et al., 2019a], a human pose estimation network. Other three works [Huang et al., 2021a,b, 2022] provided results based on different CNN structures.

To improve model performance, ten works modified the CNN structure by attention modules, which assigned varying degrees of importance (weights) to different parts of the input by learnable parameters, allowing the model to selectively focus on specific regions of an image. Traditional attention mechanisms can be classified into channel-wise [Du et al., 2022, Wang et al., 2022e, Gajbhiye et al., 2022, Pahwa et al., 2021] and spatial-wise [Pahwa et al., 2021, Jia et al., 2021], which allocate different weights to the various channels and spatial positions of the inputs respectively. In addition, Li et al. [2023b] and Wang et al. [2024a] utilized the idea of the class activation map [Zhou et al., 2016] to obtain weights. Yan et al. [2022] initially extracted image patch features, clustered them using an unsupervised method, and then weighted the cluster results. Experimental results show that attention mechanism allows models to pay more attention to the lesions than irrelevant background. With the rise of the Transformers [Vaswani et al., 2017], multi-head attention has become a potent method for information interaction. Wang et al. [2023c] first extracted regions of interest from the frontal view and then employed multi-head attention to fuse information between the frontal and lateral views with the regions. This approach introduced regions of interest into model training to improve model performance.

For Transformer architecture, most of them leverage a standard Transformer encoder, while Li et al. [2023d] argued that aligning images and text posed a challenge due to the continuous nature of images and the discrete nature of text; therefore, they improved the model performance by using a discrete variational autoencoder [Ramesh et al., 2021] to obtain discrete visual tokens. Other works improved the

model performance by modifying the self-attention module. Three works [Wang et al., 2022e, Lin et al., 2023, Wang et al., 2023d] added high-order interactions among three inputs of the Transformer attention module. Two works [Miura et al., 2021, Wang et al., 2022e] were inspired by the memory-augmented attention [Cornia et al., 2020] and extended the keys and values with additional plain learnable vectors to record more information. Li et al. [2022b] introduced a learnable parameter in the attention operation. Wang et al. [2023d] modified the encoder by including additional input tokens. These tokens were named ‘expert tokens’ to emulate the “multi-expert joint diagnosis” methodology.

Auxiliary task for feature extraction Auxiliary tasks aim to provide additional supervision signals to the feature extractor, enabling it to extract information relevant to report generation from images. These tasks mainly include classification (22 papers), graph construction (10 papers), embedding comparison (10 papers), and detection/segmentation (7 papers). Each of them is introduced in detail below.

Classification: The most common auxiliary task used in the reviewed papers is classification referring to assigning images to predefined categories. The predefined categories primarily include medical tags [Gajbhiye et al., 2022, Kaur and Mittal, 2022b, Wang et al., 2022e, Hou et al., 2021b, Du et al., 2022, You et al., 2022, Alfarghaly et al., 2021] and disease labels [Liu et al., 2021e, Zhou et al., 2021, Wang et al., 2022d, Yang et al., 2023, Zhang et al., 2023b, Wang et al., 2024a, Jin et al., 2024, Hou et al., 2021b]. The medical tags are from standard medical vocabularies including hundreds of labels, such as anatomical structures and pathological signs. They are provided by manual annotations or auto annotation tools (e.g., NIH MTI web API ² and RadGraph [Jain et al., 2021]). Disease labels are provided by auto annotation tools (e.g., CheXpert [Irvin et al., 2019] and CheXbert [Smit et al., 2020]). Compared to disease labels, medical tags offer a more comprehensive range of information. However, to the best of our knowledge, there is no literature that supports the superiority of medical tags over disease labels. Perhaps due to the extensive scope covered by medical tags, deep learning models face challenges in acquiring such rich knowledge. Zhou et al. [2021] incorporated 32 additional labels for lesion location, size, and shape (e.g., “upper/lower” and “patchy”) into the disease label set, observing a slight improvement in model performance.

Other notable categories used in the reviewed papers include matching status [Li et al., 2023a], local properties [Yang et al., 2021a], report cluster results [Li et al., 2022a], and fix answer categories [Tanwani et al., 2022]. Li et al. [2023a] predicted the matching status of a given image-report pair. Yang et al. [2021a] devised localized property labels for breast ultrasound images, such as tumor morphology, to facilitate the identification of properties that are challenging to be discerned in low-resolution images. Li et al. [2022a] first conducted unsupervised clustering on the ground truth report, subsequently utilizing the resultant clusters as labels. This auxiliary task yielded a marked improvement in text generation performance. Tanwani et al. [2022] considered the report generation as a question-answer task, and the classifier was designed for fixed answer categories. In addition, for a detection auxiliary task, classifiers need to be applied to identify attributes of detected regions (e.g., ‘right lung’). This paragraph eschews such cases to circumvent redundancy.

Graph construction: Graph construction aims at introducing prior knowledge into the report generation process. The knowledge graph in this section differs from that in Section 3.1. Here, node features are extracted from images, and edges are defined as parameters in graph convolution networks. In contrast, the node and edge information in the input knowledge graphs is derived from non-image data. A classical method was proposed by Zhang et al. [2020] and yielded promising outcomes. A knowledge graph was constructed firstly based on insights provided by domain experts, where nodes represented major abnormalities and major organs, and bidirectional connections linked nodes that were related to each other. To initialize nodes features, a spatial attention module was introduced after the CNN backbone using 1×1 convolution layers and softmax layers. The number of channels matched the number of nodes. The nodes’ initial embedding was derived as attention-weighted feature maps. Then graph convolution layers were employed to disseminate information throughout the graph, followed by two branches for classification and report generation. First, the classification branch was trained, and subsequently, parameters in both the CNN backbone and the graph convolution layers were frozen, only the report generation decoder was trained. Six works [Liu et al., 2021b,d, Cao et al., 2022, Wang et al., 2022c, Yan, 2022, Zhang et al., 2023b] utilized this method [Zhang et al., 2020]. Wang et al. [2022c] expanded the graph [Zhang et al., 2020] by incorporating information from a radiology terms corpus named Radiology Lexicon (RadLex)³ [Langlotz, 2006]. As the number of graph nodes increased, the model performance initially improved, peaked at 40 nodes, and then declined, with a noticeable decrease at 60 nodes. Liu et al. [2021d] constructed a large graph based on the MIMIC-CXR dataset. The nodes represented frequent clinical abnormalities and the edges represented the co-occurrence situation of different abnormalities. In addition, Li et al. [2023b] used the disease prediction results to obtain the node features. The nodes were classification probabilities, with learnable edge weights.

Another graph reconstruction method aims at reconstructing triplets that are in the form of (entity1, relationship, entity2), such as (opacity, suggestive of, infection). Three works [Dalla Serra et al., 2022, 2023b, Li et al., 2022b] firstly predicted the triplets and then generated reports based on them. The experimental results show that using triplets alone for report generation is ineffective; combining them with features extracted from images is necessary for better results.

Embedding comparison: Embedding comparison refers to constraining the consistency of different features in intermediate layers, thereby guiding the learning process. The comparison in reviewed papers is mainly applied between features extracted from images and real reports [Najdenkoska et al., 2021, 2022, Zhou et al., 2021, Yang et al., 2021b, Chen et al., 2022, Wang et al., 2021, 2022d, Yang et al., 2023]. Experimental results show that the supervision signals from real text enable extracted visual features carry richer semantic

²<https://ii.nlm.nih.gov/MTI/index.shtml>

³<http://www.radlex.org/>

information, facilitating more effective translation into radiology reports. Four works [Wang et al., 2021, Zhou et al., 2021, Wang et al., 2022d, Yang et al., 2023] utilized a triple loss function to compel the image-text paired features to be closer to a latent space than the unpaired ones. Najdenkoska et al. [2021, 2022] inspired by the Auto-Encoding Variational Bayes [Kingma and Welling, 2013]. They used real reports to obtain a latent space during training and generated reports based on this space. The image extractors were enabled to capture features from images that closely resemble those found in real reports. Other two works [Yang et al., 2021b, Chen et al., 2022] used the Term Frequency and Inverse Document Frequency (TF-IDF) to extract important information from real reports as supervision signals. TF-IDF is a statistical measure assessing a word's importance by considering its frequency in a specific document and its rarity across the entire document set.

In addition, to produce reports for abnormalities not seen during training, Sun et al. [2022] initially linearly projected visual features to semantic features, and extracted semantic features of labels by the BioBert model [Lee et al., 2020]. Consistent constrain was applied between two similarity: 1) the similarity between pairwise elements in the semantic features from visual features; and 2) the similarity between the semantic features from visual features and the semantic features from labels. Zhang et al. [2023b] integrated semi-supervised learning into report generation using two networks. They first applied different types of noise to an input image to create two variations, which were then fed into the two networks. An auxiliary loss function was employed to ensure consistency in the extracted visual features.

Detection/segmentation: Object detection locates and identifies objects or patterns within an image, focusing on determining their presence and position. Segmentation divides an image into meaningful regions by identifying and separating objects based on specific characteristics. Both processes enhance the model's understanding of the image by object recognition and region extraction, and can improve the model's interpretability by linking the detection/segmentation results with generated sentences. The detection/segmentation regions can be anatomical regions [Tanida et al., 2023, Dalla Serra et al., 2023b,a, Wang et al., 2023c, Han et al., 2021, Gu et al., 2024] and abnormal regions [Sun et al., 2022]. No literature compares the impact of detection and segmentation tasks on report generation results. However, a publicly available dataset named Chest ImaGenome (see Section 4) offers detection annotations, making them easier to be acquired than segmentation annotations.

In addition, the outputs of auxiliary tasks can provide valuable information such as disease labels, therefore, inputting them into the following generation network is a common choice [Alfarghaly et al., 2021, Hou et al., 2021b, Singh et al., 2021, Yang et al., 2021a, You et al., 2021, Zhou et al., 2021, Du et al., 2022, Jia et al., 2022, Kaur and Mittal, 2022b, Sun et al., 2022, Wang et al., 2022a,e, Yan et al., 2022, You et al., 2022, Tanida et al., 2023, Li et al., 2022b, Jin et al., 2024]. For example, Zhou et al. [2021] sent the semantic word embeddings of the predicted findings from the classifier to the report generation decoder.

Contrastive learning for feature extraction Contrastive learning is a self-supervised learning method to improve the representational capacity of models, which allows models to minimize the distance among positive pairs and maximize it for negative ones. It can be used to train feature extractors [Wang et al., 2022e, Lin et al., 2023, Wu et al., 2022, Wang et al., 2023b]. Lin et al. [2023] utilized a classical contrastive learning method named Momentum Contrast [He et al., 2020], where different views or augmented versions of the same image were considered as positive pairs. Another representative contrastive learning work is the Contrastive Language-Image Pre-training (CLIP) model [Radford et al., 2021]. It connects textual and visual information by directly training on a vast dataset consisting of image-text pairs. Wang et al. [2022e] directly employed it for image feature extraction and Wu et al. [2022] applied the idea of CLIP to train the feature extractors on the training dataset. Wang et al. [2023b] however argued that previous works treated the entire report as input, overlooking the distinct information contained within individual sentences. This oversight could result in incorrect matching of image-text pairs. Therefore, they proposed phenotype-based contrastive learning. This method involved randomly initializing a set of vectors as phenotypes, allowing sentences and visual embeddings to interact with them, and finally conducting contrastive learning between the processed embeddings. The results outperformed previous contrastive learning methods in report generation.

Contrastive learning also can be part of the training loss [Tanwani et al., 2022, Wang et al., 2022a, Li et al., 2023a, Liu et al., 2023b], and can be applied between visual and textual features (i.e. image-text pairs) [Tanwani et al., 2022, Li et al., 2023a, Liu et al., 2023b], or be applied based on labels, treating samples with shared labels as positives and those without any common labels as negatives [Wang et al., 2022a]. Their ablation study demonstrated a significant improvement in results compared to standard contrastive loss [Wang et al., 2022a].

Contrastive attention is another method to utilize contrastive learning. Liu et al. [2021c] designed a contrastive attention model to extract abnormal region features by comparing input samples with normal cases. Similar features shared between the input and normal cases were subtracted from the input image feature, and the remaining feature was then concatenated with the original feature. Song et al. [2022] argued that the contrastive technique [Liu et al., 2021c] did not consider historical information, therefore they proposed a module based on similarity retrieval technique to obtain similar images from the training dataset. The image features were processed by enlarging different features between inputs and the similar retrieved images.

Memory metric for feature extraction Using a memory metric for image feature extraction assumes the presence of similar features in various medical images. Memory metrics are employed to record and transmit the similarity information during training [Chen et al., 2022, Yan, 2022]. Typically, an $n \times n$ matrix is randomly initialized, where n represents the number of metric rows. Then, at each training step, the matrix is updated based on the visual features and the previous metrics. The memory metric used in this section is consistent

with the metric used in the memory-driven transformer discussed in Section 3.5, with one being applied to images and the other to the generated reports.

3.3.2 Non-imaging-based feature learning

Most non-imaging data is presented in the form of text. Before fusion with image data, text data needs to be embedded. We first introduce a widely-used basic text embedding technique, the lookup table. This table assigns a unique index to each word or character, which is used to look up a pre-trained word vector or character vector. In addition to the basic method, additional feature extraction can be performed on these vectors to enhance their representation capabilities.

Transformer-based models such as BERT and its variants have emerged as mainstream methods for feature extraction across various textual data, such as terminology [Liu et al., 2021e, Cao et al., 2022, 2023, Liu et al., 2021b, Xue et al., 2024, Liu et al., 2023b, Li et al., 2023c], real text reports [Liu et al., 2021b, 2023b, Li et al., 2023c, Jin et al., 2024], knowledge graphs [Yang et al., 2022, Huang et al., 2023, Li et al., 2023a, Xu et al., 2023], and questionnaires [Tanwani et al., 2022, Pellegrini et al., 2023], and have achieved good results.

Several methods are designed for a specific type of input. Li et al. [2023c] used the TF-IDF to re-weight terminology embeddings. The re-weighted approach alleviated the issue of data imbalance, resulting in performance enhancement. Clinical information can be processed by a pre-trained feature extractor named BioSentVec [Zhou et al., 2021, Chen et al., 2019]. For the knowledge base, Yang et al. [2022] used a knowledge graph embedding model named RotatE [Sun et al., 2019b] to obtain entity embeddings and relation embeddings from the RadGraph. Besides using the entire RadGraph as input, two works combined the real reports with RadGraph to extract case-related information from real reports and queried related information from the RadGraph [Yang et al., 2022, Li et al., 2023a]. Alternatively, Li et al. [2023c] considered RadGraph as an annotation tool for extracting entities and positional information from real reports. Other two works [Xu et al., 2023, Huang et al., 2023] utilized classification results to process the self-built graph and extracted case-related information. The experimental results substantiate the beneficial impact of incorporating case-related knowledge on report generation, particularly evident when integrating real reports with the knowledge base. In addition, age and gender information are not text data and are generally encoded as one-hot vector [Zhou et al., 2021].

3.4 Multi-modal feature fusion and interaction

Feature fusion and interaction refer to the integration of multi-modal data from inputs or auxiliary tasks. This step has two purposes. First, visual and textual features from disparate domains present challenges for model learning. By fusing and facilitating interaction between these features, the domain gap can be narrowed, thereby enhancing network learning. Second, the image regions should align with the sentences in the reports. This correspondence can be learned through fusion and interaction. In the auxiliary task of embedding comparison (see Section 3.3.1), semantic features extracted from real reports are used to supervise the learning of image features. However, this approach differs from multi-modal feature fusion. The objective of embedding comparison is to enhance image features, without incorporating non-image features into the generator. Instead, the fused features in this section are forwarded to the generator.

The most straightforward approach for feature fusion and interaction is feature-level operation including the concatenation, summation, or multiplication of multimodal features (13 works). However, the feature-level operation could be too simple to enable sufficient interaction. Therefore, neural network-based methods are leveraged, such as LSTMs (2 works) and the multi-head attention mechanism (27 works). While this approach facilitates convenient feature fusion, its lack of specific design for multi-modality data fusion leads to limited effectiveness in interaction.

We would like to highlight a memory metric-based method proposed by Chen et al. [2021]. It significantly enhanced the performance of the report generation system by facilitating feature interaction. A metric was initialized randomly. Image features, text features from generated tokens, and memory metric features were then projected into the same space. Subsequently, distances between image features and memory metric features, as well as text features and memory metric features, were calculated. The top K metric features with the closest distances to the image or text were selected, respectively. These selected features were then weighted based on these distances and were fed back into an encoder-decoder structure. Two studies [Qin and Song, 2022, You et al., 2022] followed this method. Wang et al. [2022a] modified it in two ways: 1) they initialized the matrix by visual and textual features; 2) the cross-modal interaction occurred only among cases with the same label. These two modifications both resulted in a notable improvement. Li et al. [2023d] contended that the methods mentioned lack explicit constraints for cross-modal alignments. They considered orthonormal bases as the metric and input them along with visual or textual features, into multi-head attention modules. Then the outputs of attention modules were processed by a self-defined gate mechanism. A triplet matching loss was utilized to align the processed visual and textual features. This method slightly improved the results.

3.5 Report generation

The last step is report generation, which utilizes extracted features from earlier steps to produce the final reports. The generation methods mainly include decoder-based techniques (Section 3.5.1), retrieval-based techniques (Section 3.5.2), and template-based techniques

(Section 3.5.2). In addition, the development of large language models has made it possible to utilize them to enhance the quality of generated reports. It is discussed in Section 3.5.3

3.5.1 Decoder-based techniques

The decoder decodes the extracted representation of inputs and generates a descriptive report. The mainstream architectures include LSTM [Hochreiter and Schmidhuber, 1997] and Transformer. Compared to LSTM, the Transformer processes the entire sequence simultaneously rather than sequentially. Therefore, the Transformer allows for more efficient parallelization during training and can capture long-range dependencies. In the 89 reviewed papers, the Transformer tends to replace LSTM. Fifty-five works utilized the Transformer as a decoder and only 23 of them utilized LSTMs (12 works) or hierarchical LSTMs (11 works). For the papers published in 2023 and 2024, all encoder-decoder structures used the Transformer as their decoders. There are two ways to modify the decoder and improve model performance.

Shortcut connections: Connecting different layers in networks can be considered as a promising way to enhance the flow of information in both forward and backward propagation [Mirikharaji et al., 2023]. The U-connection [Huang et al., 2023] and meshed connection [Miura et al., 2021, Lee et al., 2022, Cornia et al., 2020] are added between encoder and decoder, resulting in a similar performance enhancement [Huang et al., 2023].

Memory-driven Transformer: We would like to highlight the Memory-driven Transformer (R2Gen) proposed by Chen et al. [2020]. It has been increasingly popular in recent years. The R2Gen introduces a memory module and a memory-driven conditional layer normalization module into the Transformer decoder architecture. The design of the memory module hypothesizes that diverse images exhibit similar patterns in their radiological reports, thereby serving as valuable references for each other. Building a memory matrix can capture this pattern and transfer it during training. Specifically, similar to that in the section 3.3.1, a matrix is randomly initialized and is updated using the gate mechanism based on the matrix from the last step and generated reports. The layer normalization is designed to integrate the outputs of the memory module into the decoder.

Eight works directly utilized the R2Gen as their decoder. In addition, the design of the memory module and layer normalization inspired subsequent works [Xue et al., 2024, Jia et al., 2021, Zhang et al., 2023a]. It is noted that the novel utilization of the memory module by Zhang et al. [2023a] integrates ground truth reports into the training process, leading to successful outcomes.

3.5.2 Retrieval-based and template-based techniques

Retrieval-based techniques generate reports by selecting existing sentences from a large corpus and the selection is typically based on similarity comparison [Endo et al., 2021, Ramesh et al., 2022, Jeong et al., 2024]. Initially, text and image encoders are trained using a contrastive method, such as the CLIP [Radford et al., 2021]. The textual features of sentences in a corpus and the visual features of an input image are extracted by the encoders. The visual features are then compared with all textual features in the corpus. The top k sentences with the maximum similarity score are selected for the predicted report. In addition, Jeong et al. [2024] added a multimodal encoder after the retrieval process to calculate the image-text matching scores between the input image and the retrieved sentences. A filter was applied based on the score to remove entailed or contradicted sentences.

Other retrieval-based techniques do not follow the above process. Kong et al. [2022] treated the report generation in two steps sentence retrieval and selection. They first retrieved a candidate sentence set from the training datasets with far more sentences than a standard medical report and then selected the sentences by a classifier. Zhang et al. [2022] proposed a retrieval method based on a hashing technique, which mapped multi-modal data with the same label into a shared space.

Template-based methods typically start with the diagnosis of diseases, and then pre-defined sentences are selected based on the diagnosis results. These selected sentences are concatenated to produce reports [Pino et al., 2021]. Abela et al. [2022] argued that this method was limited by exact labels, therefore they retrieved template sentences by class probabilities and different thresholds corresponding to different descriptions.

3.5.3 Large language model to assist report generation

With the emergence of ChatGPT [OpenAI, 2023], its powerful language abilities made researchers eager to harness the power of large language models to aid in report generation. However, employing it directly within the medical domain led to unsatisfactory outcomes [Tu et al., 2024, Yan et al., 2023, Sun et al., 2023]. Two works [Selivanov et al., 2023, Wang et al., 2023a] initially predicted report-related information such as diseases, lesion regions, and visual features, and generated preliminary reports. Subsequently, they employed pre-trained large language models, e.g., ChatGPT [Wang et al., 2023a] or GPT-3 [Brown et al., 2020, Selivanov et al., 2023, Wang et al., 2023a] to improve the preliminary report with the predicted information and produced the final reports. The results have been moderately improved. Exploration of large language models in the field of medical report generation still requires further investigation, which is discussed in Section 7.4.

3.6 Training strategy

Training strategy refers to the techniques used to train neural network models. Traditionally, models are trained by minimizing various loss functions. Therefore, this section begins by introducing different loss functions (Section 3.6.1), followed by a discussion on reinforcement learning (Section 3.6.2), and the curriculum learning’s application to the report generation task (Section 3.6.3).

3.6.1 Loss functions

The mainstream loss function for report generation is the cross-entropy loss based on the generated sentences and the ground-truth sentences. Cross-entropy loss can be re-weighted based on term frequency [Gajbhiye et al., 2022], TF-IDF [Wang et al., 2022d] or uncertainty [Wang et al., 2024b] to mitigate model bias or handle challenging cases. In addition, Pandey et al. [2021] utilized cycle-consistency loss [Zhu et al., 2017] to generate reports. The core idea is that a report and its corresponding image share the same information, hence they can be used to generate each other.

The application of an auxiliary loss function can provide additional supervision signals, further enhancing model performance. Two works Wang et al. [2021], Li et al. [2022a] applied an additional constraint between features extracted from the generated and real reports. Zhang et al. [2023b] created two different versions of an input image by adding noise and feeding them into two networks. An auxiliary loss function ensures the consistency of the outputs produced by the two generators. Wang et al. [2024a] obtained two discriminative regions in an image from the generated words and visual classifier separately, then enforced the consistency between them.

3.6.2 Reinforcement learning

Reinforcement learning involves training an agent to make optimal decisions through trial and error, aiming to maximize targeting rewards. It offers a method to update the model parameters based on non-differentiable reward functions [Messina et al., 2022]. Evaluation metrics can be considered as rewards, such as CIDEr [Kaur and Mittal, 2022b], BLEU [Qin and Song, 2022, Gu et al., 2024], METEOR [Qin and Song, 2022], ROUGE [Qin and Song, 2022], BERTScore [Miura et al., 2021], F1 score [Miura et al., 2021], and accuracy [Hou et al., 2021b]. In addition, Hou et al. [2021b] trained a language fluency discriminator using the ground truth and generated reports, and then utilized the discriminator to provide rewards.

3.6.3 Curriculum learning

Liu et al. [2021a] utilized curriculum learning [Platanios et al., 2019] to classify training instances and trained a model from simple to complex samples. Data pairs were evaluated based on image heuristics, image confidence, text heuristics, and text confidence. Image heuristic evaluated the similarity between input images and normal images. Image confidence indicated the confidence of a classification model. The report heuristic was related to the number of abnormal sentences, and report confidence was evaluated by the negative log-likelihood loss [Xu et al., 2020].

4 Datasets

Datasets play a crucial role in the development of report-generation models. Abundant and diverse training data can improve the model’s accuracy and generalizability. Moreover, a suitable test dataset makes it realistic to test the model’s performance in a practical scenario. In this section, we selected 11 public medical image-report datasets utilized in the reviewed articles to provide a comprehensive introduction of popular and newly collected datasets, see Table 1. The usage of datasets in each article is shown in Table A1 in Appendix A. The datasets primarily focus on the lung, including X-ray [Demner-Fushman et al., 2016, Johnson et al., 2019a,b] and CT [Li et al., 2020, Liu et al., 2021e]. In addition, there are also publicly available datasets on eye scans [Huang et al., 2021b, Lin et al., 2023, Li et al., 2021] and breast scans [Yang et al., 2021a]. The concentration of medical report generation efforts on chest X-rays can be attributed, in part, to the accessibility of large-scale publicly available datasets.

The most popular datasets are the Indiana University Chest X-Ray Collection (IU X-Ray) [Demner-Fushman et al., 2016] and the MIMIC Chest X-ray (MIMIC-CXR) [Johnson et al., 2019a,b]. The IU X-ray contains 7470 images of frontal and lateral X-rays and 3955 reports with manual annotation based on the MeSH codes⁴ and the RadLex codes. These codes encompass standard medical terminology, such as anatomical structures, diseases, pathological signs, foreign objects, and attributes, as defined by authoritative institutions. For deep learning methods, the size of the IU X-RAY is insufficient, while the collection of MIMIC-CXR alleviates this problem [Messina et al., 2022]. It consists of 377,110 images and 227,827 reports, and has been multi-labeled by automatic tools according to 14 disease categories. An image-report sample from the MIMIC-CXR dataset is shown in the Figure 4. The indication, technique, and comparison provide fundamental information for a Chest X-ray test. The automation of radiology report generation targets the findings and impressions sections. The findings section provides a detailed description of the entire image, while the impressions section summarizes these observations. The follow-up work provides MIMIC-CXR with richer label information. The Chest ImaGenome dataset [Wu et al., 2021]

⁴<https://www.nlm.nih.gov/mesh/meshhome.html>

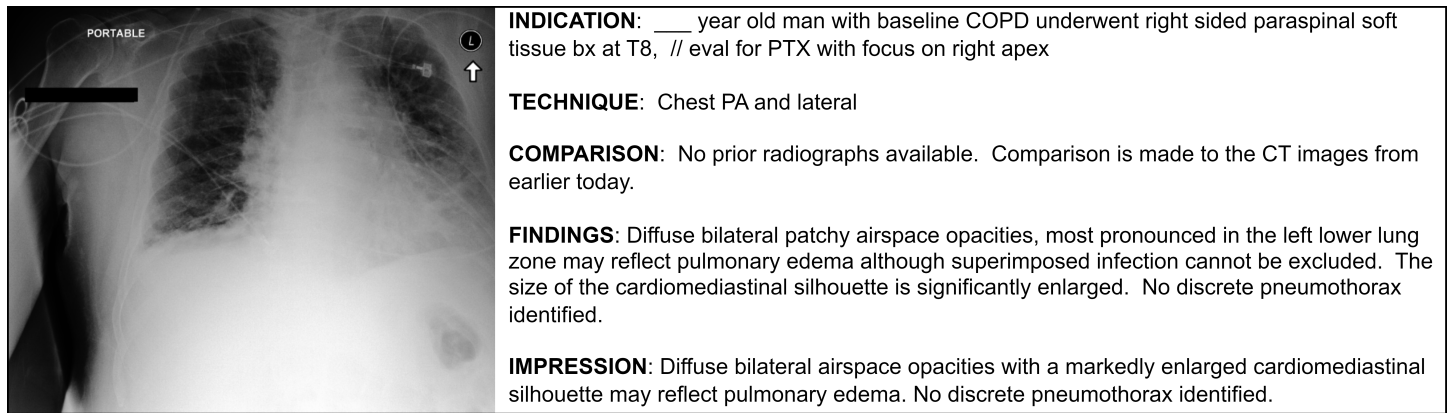


Figure 4: A sample from the MIMIC-CXR dataset. The left is the Chest X-ray image and the right is its corresponding radiology report.

Table 1: Public datasets for medical report generation.

Name	Image type	Report type	Images	Reports	Patients	Used by
IU X-Ray [Demner-Fushman et al., 2016]	Chest X-ray	Unstructured	7,470	3,955	3,955	67 works
MIMIC-CXR [Johnson et al., 2019a,b]	Chest X-ray	Unstructured	377,110	227,827	65,379	59 works
Chest ImaGenome [Wu et al., 2021]	Chest X-ray	Unstructured	242,072	217,013	–	4 works
COV-CTR [Li et al., 2020]	Chest CT	Unstructured	728	728	–	4 works
DeepEyeNet [Huang et al., 2021b]	FA, CFP	Unstructured	15,709	15,709	–	3 works
FFA-IR [Li et al., 2021]	FFA	Unstructured	1,048,584	10,790	–	2 works
Chinese COVID-19 CT [Liu et al., 2021e]	Chest CT	Unstructured	1,104	368	96	1 work
BCD2018 [Yang et al., 2021a]	Breast Ultrasound	Unstructured	5,349	5,349	–	1 work
Retina ImBank [Lin et al., 2023]	FP, OCT, FFA, FAF, ICG, and red-free filtered fundus images	Unstructured	18,788	18,788	–	1 work
Retina Chinese [Lin et al., 2023]	FP, FFA, and ICG	Unstructured	57,498	57,498	–	1 work
Rad-ReStruct [Pellegrini et al., 2023]	Chest X-ray	Structured	3,720	3,597	3,597	1 work

is based on the anteroposterior and posteroanterior view Chest X-ray images in the MIMIC-CXR dataset. It provides an anatomy-centered scene graph for each image, including anatomical location and relation annotations. The annotations are generated through two automated pipelines, and a separate dataset of 500 manually annotated cases is also provided for testing.

Increasing attention has been paid to the collection of ophthalmic image-report pairs [Huang et al., 2021b, Li et al., 2021, Lin et al., 2023]. Ophthalmic image has lots of modalities, such as Fluorescein Angiography (FA), Fundus Fluorescein Angiography (FFA), Color Fundus photography (CFP), fundus photograph (FP), optical coherence tomography (OCT), fundus autofluorescence (FAF), Indocyanine Green Chorioangiography (ICG), and red-free filtered fundus images. Most of retinal datasets are based on one or two modalities and the last released Retina ImBank dataset is the first multi-modality retinal image-text dataset [Lin et al., 2023]. Some datasets provide additional labels for each image, such as lesion boundary [Li et al., 2021], lesion category [Huang et al., 2021b, Li et al., 2021], and keywords [Huang et al., 2021b].

All the above datasets provide unstructured reports. Recently, Pellegrini et al. [2023] released a structured report dataset named Rad-ReStruct based on the IU-XRAY. In clinical practice, generating structured reports typically requires doctors to answer a sequence of questions [Pellegrini et al., 2023]. Therefore, Pellegrini et al. [2023] designed a structured report template with a series of single- or multi-choice questions based on topic existence (e.g., Are there any diseases in the lung?), element existence (e.g., Is there an opacity in the lung?), and attributes (e.g., What is the degree?). They then integrated the IU-XRAY report data into the template using its annotated MeSH and RadLex codes.

5 Evaluation

Accurate assessment of the quality of generated reports is crucial for measuring model performance. The quality of generated reports can be evaluated both quantitatively and qualitatively. Quantitative methods check the text quality and medical correctness of the generated report by natural language evaluation metrics (Section 5.1) and medical correctness metrics (Section 5.2), respectively. Qualitative

Table 2: The quantitative and qualitative evaluation methods for medical report generation.

Metrics	Description	Used by
Natural language-based metrics		
BLEU [Papineni et al., 2002]	A precision-based metric that measures the n-gram overlapping of the generated text and ground truth text.	84 works
ROUGE-L [Lin, 2004]	A F1-like metric that computes a weighted harmonic mean of precision and recall based on the longest common subsequence.	75 works
METEOR [Banerjee and Lavie, 2005]	A F1-like metric that computes a weighted harmonic mean of unigram precision and recall. It is an extension of BLEU-1.	57 works
CIDEr [Vedantam et al., 2015]	The cosine similarity between generated text and ground truth text based on the TF-IDF.	41 works
S_{emb} [Endo et al., 2021]	Sending ground truth report and generated report into a textual feature extractor and calculating the cosine similarity between their embeddings from the last layer.	2 works
%Novel [Van Miltenburg et al., 2018]	The percentage of generated descriptions that are not present in the training data.	1 work
Medical correctness-based metrics		
Clinical Efficacy [Chen et al., 2020, Liu et al., 2019]	Calculate accuracy, precision, recall, and F1 score based on observations extracted from reference reports and generated reports by automated system.	34 works
MIRQI [Zhang et al., 2020]	Calculate precision, recall, and F1 score based on graph comparison. The ground truth and generated reports are automatically analysed to construct a sub-graph from a defined abnormality graph.	2 work
nKTD [Zhou et al., 2021]	Calculate the Hamming distance based on observations extracted from reference reports and generated reports by the CheXpert Labeller.	1 work
Human-based evaluation		
Comparison	Generate reports by two different models and allow senior radiologists to find which report is better.	12 works
Classification	Radiologists categorize the produced reports as accurate, missing details, and false reports.	1 work
Error scoring	Radiologists assess the error severity of baseline, model generated, and reference reports.	1 work
Grading	Radiologists need to assign a 5-point scale grade to two types of generated reports, in accordance with clinical standards.	1 work

evaluation is normally performed by human experts and they provide overall evaluation for the generated reports (Section 5.3). Table 2 summarizes the description of evaluation methods introduced in this section. The usage of evaluation methods in each article is shown in Table A1 in Appendix A.

5.1 Natural language-based evaluation metrics

Natural language evaluation metrics are from natural language processing tasks and measure the general text quality of generated reports. In the reviewed papers, the most popular metrics are BLEU [Papineni et al., 2002], ROUGE-L [Lin, 2004], METEOR [Banerjee and Lavie, 2005], and CIDEr [Vedantam et al., 2015], which are based on n-gram matching between reference reports and generated reports. The model is deemed superior with an increased number of matches. Among them, the BLEU is the earliest and proposed a modified precision method. When evaluating the quality of radiology report generation, we typically opt for BLEU-1, BLEU-2, BLEU-3, and BLEU-4 metrics. The n in BLEU-n means the calculation is based on n-gram. The METEOR is an extension of BLEU-1 and introduces recall into evaluation. The ROUGE-L also considers precision and recall based on the longest common subsequence between reference and generated text. The CIDEr adopts the TF-IDF. The TF-IDF vectors weigh each n-gram in a sentence, and then the cosine similarity is calculated between the TF-IDF vectors of reference and generated text. When the model consistently produces the most common sentences, it can achieve notable BLEU scores. However, CIDEr can evaluate generated outputs by encouraging the appearance of important terms and punishing high-frequency vocabulary [Li et al., 2023a]. CIDEr has a popular variant CIDEr-D, which introduces penalties to generate desired sentence length and remove stemming to ensure the proper usage of word forms.

Other than n-gram matching, Endo et al. [2021] proposed a new metric S_{emb} . A pre-trained feature extractor is applied on both the ground truth and the generated reports, and the cosine similarity between extracted embeddings is calculated. This approach is used to assess whether the semantic information contained in two sentences is consistent. Another natural language metric %Novel [Van Miltenburg et al., 2018] is introduced to evaluate the diversity in image captioning.

5.2 Medical correctness metrics

Natural language evaluation metrics evaluate the similarity between produced reports and the ground truth, but cannot accurately measure whether the generated reports contain the required medical facts [Babar et al., 2021b, Messina et al., 2022]. So medical correctness metrics are proposed to pay attention to the prediction of important medical facts. Generally, an automatic labeller is applied to extract medical facts from generated and reference reports. Then different metrics are applied to these. The mainstream metric is clinical efficacy [Liu et al., 2019, Chen et al., 2020], which initially calculates precision, recall, and F1 score, and subsequently extends to accuracy [Babar et al., 2021a, Miura et al., 2021, Moon et al., 2022, Yan, 2022, Yang et al., 2022, Selivanov et al., 2023, Yang et al., 2023] and AUC [Li et al., 2023a]. Most of the works utilized CheXpert [Irvin et al., 2019] as a labeler to extract chest diseases information from ground truth reports, while seven of them [Miura et al., 2021, Yan, 2022, Wang et al., 2023a, 2024a, Dalla Serra et al., 2023b,a, Jin et al., 2024] utilized a newer labeler CheXbert [Smit et al., 2020], which has a higher performance. In addition, Pellegrini et al. [2023] generated structured reports by predicting a series of questions. They utilized macro precision, recall, and F1 score to assess all questions, along with evaluating report-level accuracy. Other metrics calculate the Hamming distance [Zhou et al., 2021] or perform graph comparison [Zhang et al., 2020] based on the extracted results.

5.3 Human-based evaluation

For qualitative assessment, the most common human-based evaluation method is comparison. In general, a set number of samples (i.e., 100/200/300) are selected from the test dataset and subsequently processed by different generated models. More than one professional clinician is responsible to compare and sort the generated reports. Five works utilized ground truth reports in this process. Two works [Miura et al., 2021, Cao et al., 2022] considered the ground truth reports as a reference. Reports were generated by different generators and the radiologists need to select which report is more similar to the reference. Dalla Serra et al. [2022] allowed experts to find 5 types of errors (i.e., hallucination, omission, attribute error, impression error, and grammatical error) in different generated reports according to the reference reports. Xu et al. [2023] asked radiologists to rank the ground truth reports and the generated reports. Qin and Song [2022] invited experts to select the most suitable report from the generated and the ground truth reports according to correctness, language fluency, and content coverage. Other expert evaluation methods are classification [Alfarghaly et al., 2021], grading [Wang et al., 2024b], and error scoring [Jeong et al., 2024].

6 Benchmark Comparison

For model comparison, it is essential to select a benchmark for an impartial evaluation. We choose the MIMIC-CXR [Johnson et al., 2019b,a](see Table 3) dataset as a benchmark to compare the model performance for two reasons. First, according to Table 1, IU-Xray and MIMIC-CXR are the most popular datasets, but IU X-ray lacks standard training-validation-test splits, leading to less comparable results [Messina et al., 2022], while MIMIC-CXR has official training-validation-test splits. Second, MIMIC-CXR is the largest image-report dataset, which provides a broader distribution of data, facilitating testing across diverse scenarios, and reducing biases commonly encountered in smaller datasets.

We endeavour to ensure equitable comparisons, but it’s important to consider the following three problems when analysing these results. First, we select the methods leveraged the official splits of the MIMIC-CXR dataset [Johnson et al., 2019b], containing 368960 images (with 222758 reports) in the training dataset, 2991 images (with 1808 reports) in the validate dataset, and 5159 images (with 3269 reports) in the test dataset. Although some papers claimed to use official splits, the total number of datasets is different. For example, the MIMIC-CXR used by Najdenkoska et al. [2022] contains 218,101 samples. These papers were excluded. In Section 3, a multitude of methodologies are highlighted. However, due to stringent screening, their absence from the comparison table does not imply inferior performance. Second, we choose BLEU, ROUGE, METEOR, CIDEr-D, precision, recall, and F1 score metrics as evaluation metric. Similar to the previous survey [Messina et al., 2022], we found that although some metrics have variants, many papers do not specify the particular version used. In that case, we assume they are consistent. Third, the generated report sections vary among different methodologies. Most articles do not explicitly specify the generated report sections, making it challenging to conduct comparative analysis.

We separate the comparison results based on the generated report section, and the completed comparison tables are provided in Table A2 in Appendix A. Table 3 shows the best and second best performances ranked for each evaluation metric. Among the 14 papers in Table 3, three of them [Song et al., 2022, Liu et al., 2023b, Jin et al., 2024] utilized multi-modality inputs. From an architectural perspective, in the encoding stage, five works utilized a pure Transformer model [Wang et al., 2022e, Kong et al., 2022, Liu et al., 2023b, Wang et al., 2023d, 2022d], another five works employed the CNN-based model [Pino et al., 2021, Song et al., 2022, Wu et al., 2022, Jia et al., 2022, Jin et al., 2024], and four works combined CNN and Transformer [Chen et al., 2021, Wang et al., 2023c, 2024a, Wu et al., 2023]. In the generation stage, most papers relied on the Transformer. In terms of technical modules, six works [Wang et al., 2022e, Jin et al., 2024, Wang et al., 2023d, Wu et al., 2023, Wang et al., 2024a, 2022d] designed auxiliary tasks and five works [Song et al., 2022, Wu et al., 2022, Wang et al., 2023d, Liu et al., 2023b, Wang et al., 2022e] used contrastive learning.

Table 3: Comparisons of the model performance on the MIMIC-CXR Dataset. B1, B2, B3, B4, R-L, C-D, P, R, and F represent BLEU-1, BLEU-2, BLEU-3, BLEU-4, ROUGE-L, CIDEr-D, precision, recall, and F1 score, respectively. **The best** and **second best** results are highlighted. All values were extracted from their papers.

Paper	B1↑	B2↑	B3↑	B4↑	R-L↑	METEOR↑	C-D↑	P↑	R↑	F↑
Findings Section										
Chen et al. [2021]	0.353	0.218	0.148	0.106	0.278	0.142	-	0.334	0.275	0.278
Pino et al. [2021]	-	-	-	-	0.185	-	0.238	0.381	0.531	0.428
Song et al. [2022]	0.360	0.227	0.156	0.117	0.287	0.148	-	0.444	0.297	0.356
Impression + Findings Section										
Wu et al. [2022]	0.340	0.212	0.145	0.103	0.270	0.139	0.109	-	-	-
Wang et al. [2022d]	0.351	0.223	0.157	0.118	0.287	-	0.281	-	-	-
Jia et al. [2022]	0.363	0.228	0.156	0.130	0.300	-	-	-	-	-
Unspecified generated sections										
Wang et al. [2023c]	0.363	0.235	0.164	0.118	0.301	0.136	-	-	-	-
Wang et al. [2024a]	0.374	0.230	0.155	0.112	0.279	0.145	0.161	0.483	0.323	0.387
Wu et al. [2023]	0.383	0.224	0.146	0.104	0.280	0.147	-	-	-	0.758
Wang et al. [2023d]	0.386	0.250	0.169	0.124	0.291	0.152	0.362	0.364	0.309	0.311
Liu et al. [2023b]	0.391	0.249	0.172	0.125	0.304	0.160	-	-	-	-
Jin et al. [2024]	0.398	-	-	0.112	0.268	0.157	-	0.501	0.509	0.476
Wang et al. [2022e]	0.413	0.266	0.186	0.136	0.298	0.170	0.429	-	-	-
Kong et al. [2022]	0.423	0.261	0.171	0.116	0.286	0.168	-	0.482	0.563	0.519

7 Challenges and Future Works

Although automated systems offer promising efficiency for clinical workflows, current methods have not produced very high-quality reports. This section evaluates the current progress in automated report generation development and identifies potential areas for improvement.

7.1 Constructing and utilizing multi-modal data

Considering report generation as a multi-modal problem is more aligned with clinical practice [Tu et al., 2024, Yan et al., 2023]. Babar et al. [2021a] have proven the ineffectiveness of simple encoder-decoder report generation models and mentioned that adding prior knowledge can be a promising method. However, the current utilization of multi-modal data remains under-explored. Firstly, the methods for non-image feature extraction and the fusion of multi-modality data are often limited and simplistic, such as using graph encoding for the knowledge base and attention mechanisms for feature fusion. Secondly, the construction of the knowledge base is imperfect. The pre-defined graph [Zhang et al., 2020] is overly simplistic. Despite Radgraph being a vast knowledge base, it is solely derived from reports, lacking the relationship between images and reports, such as organ recognition or understanding of typical radiological scenarios, which radiologists possess. The Chest ImaGenome dataset [Wu et al., 2021] provides the organ recognition annotations, alleviating the problem. Additionally, as far as we know, publicly available knowledge bases only concentrate on chest X-rays, leaving a gap in general medical knowledge databases.

7.2 Evaluation of medical correctness

Evaluating the medical correctness of generated reports is crucial for the clinical application. Compared to previous works [Messina et al., 2022, Liao et al., 2023], recent works have paid more attention to it, but still have two shortcomings. First, in the reviewed articles, medical correctness evaluation has only been applied to chest X-ray reports. Secondly, the evaluation is based on the automatic labeler of radiology reports, which are only targeted at 14 types of diseases and the average F1 score is around 0.798 [Smit et al., 2020]. Thus, improving the accuracy and scale of automatic labeling tools can help optimize the evaluation process.

7.3 Large public datasets and unified comparison benchmark

As shown in Table 1, most of the public datasets are limited in size. Deep learning-based techniques require a large amount of data. The contemporary prevalence of large language models underscores this need for extensive data volumes. Among the datasets, the MIMIC dataset is relatively large but only includes Chest X-ray data. Large datasets targeting other image modalities and diseases need to be constructed. In addition, while MIMIC-CXR is a well-established benchmark compared to IU-XRay, dataset utilization lacks standardization, complicating comparisons. We urge papers using the MIMIC dataset to define their training, validation, and testing partitions, with explicit disclosure of the filtration method, particularly for the testing dataset.

7.4 Human-AI interaction

Most papers overlook the interaction between users (e.g., clinicians or patients) and automated systems. When the system performs as an AI assistant, users may want to know the insights of the model regarding specific aspects of medical images. In the reviewed works, Tanwani et al. [2022] constructed a Visual Question Answering system for medical report generation, and Tanida et al. [2023] linked the output results to image regions using object detection, allowing users to select areas of interest and receive corresponding language explanations. Recently, dialogue systems (e.g., GPT-4 [Achiam et al., 2023], PaLM [Chowdhery et al., 2023], Gemini [Team et al., 2023]) based on large language models and large multi-modal models have shown people more possibilities for human-AI interaction. Although general large language models can provide answers to some questions in medical question answering benchmarks, their deployment in clinical settings remains unfeasible due to safety concerns within the medical domain [Yan et al., 2023, Saab et al., 2024].

To enable dialogue systems to comprehend medical knowledge, fine-tuning the model with medical data is an intuitive approach, such as LLaVA-Med [Li et al., 2024] and Med-PaLM 2 [Singhal et al., 2023]. However, they did not test the model’s performance on the report generation task. Saab et al. [2024] proposed Med-Gemini, a series of highly proficient multi-modal models tailored specifically for the medical domain. They intuitively showed the interactive report generation process for a normal case, while lacking quantitative results to evaluate report generation performance. Exploring the direction of report generation with human-AI interaction holds significant promise. Additionally, fine-tuning large models demands substantial GPU resources, making efficient methods crucial.

7.5 Standardized report generation

Most of the existent methods focused on unstructured report generation, while structured reporting has several advantages, such as saving time [Hong and Kahn, 2013, Nobel et al., 2022], preventing errors, decreasing communication expenses linked to ambiguous natural language. Recently, Pellegrini et al. [2023] developed a structured template and released a related dataset. This promising start could pave the way for further exploration in this direction.

8 Conclusions

In this study, we have conducted a detailed technical review of 89 papers on automatic medical report generation published in the years 2021, 2022, 2023, and 2024 to showcase both mainstream and novel techniques. Our particular focus lies on the utilization and fusion of multi-modality data. The analysis of methods is structured based on the components of the report generation pipeline, presenting the key techniques for each component. Additionally, we provide a summary of the current publicly available datasets and evaluation methods, encompassing both quantitative and qualitative assessments. Subsequently, we compare the results from a subset of the 89 papers under the same experimental setting. Finally, we outline the current challenges and propose future directions for medical report generation. Overall, sustained progress is needed to produce standardized and clinically accurate reports. This survey aims to offer a comprehensive overview of report-generation techniques, emphasize critical issues, and assist researchers in promptly grasping recent advancements in the field to build more robust systems for clinical practice.

References

- Brandon Abela, Jumana Abu-Khalaf, Chi-Wei Robin Yang, Martin Masek, and Ashu Gupta. Automated radiology report generation using a transformer-template system: Improved clinical accuracy and an assessment of clinical safety. In *AI 2022: Advances in Artificial Intelligence: 35th Australasian Joint Conference, AI 2022, Perth, WA, Australia, December 5–8, 2022, Proceedings*, pages 530–543. Springer, 2022.
- Josh Achiam, Steven Adler, Sandhini Agarwal, Lama Ahmad, Ilge Akkaya, Florencia Leoni Aleman, Diogo Almeida, Janko Altschmidt, Sam Altman, Shyamal Anadkat, et al. Gpt-4 technical report. *arXiv preprint arXiv:2303.08774*, 2023.
- Omar Alfarghaly, Rana Khaled, Abeer Elkorany, Maha Helal, and Aly Fahmy. Automated radiology report generation using conditioned transformers. *Informatics in Medicine Unlocked*, 24:100557, 2021.
- Zaheer Babar, Twan van Laarhoven, and Elena Marchiori. Encoder-decoder models for chest x-ray report generation perform no better than unconditioned baselines. *Plos one*, 16(11):e0259639, 2021a.
- Zaheer Babar, Twan van Laarhoven, Fabio Massimo Zanzotto, and Elena Marchiori. Evaluating diagnostic content of ai-generated radiology reports of chest x-rays. *Artificial Intelligence in Medicine*, 116:102075, 2021b.
- Satanjeev Banerjee and Alon Lavie. Meteor: An automatic metric for mt evaluation with improved correlation with human judgments. In *Proceedings of the acl workshop on intrinsic and extrinsic evaluation measures for machine translation and/or summarization*, pages 65–72, 2005.
- Djamila-Romaissa Beddiar, Mourad Oussalah, and Tapio Seppänen. Automatic captioning for medical imaging (mic): a rapid review of literature. *Artificial Intelligence Review*, 56(5):4019–4076, 2023.

- Tom Brown, Benjamin Mann, Nick Ryder, Melanie Subbiah, Jared D Kaplan, Prafulla Dhariwal, Arvind Neelakantan, Pranav Shyam, Girish Sastry, Amanda Askell, et al. Language models are few-shot learners. *Advances in neural information processing systems*, 33: 1877–1901, 2020.
- Yiming Cao, Lizhen Cui, Fuqiang Yu, Lei Zhang, Zhen Li, Ning Liu, and Yonghui Xu. Kdtnet: medical image report generation via knowledge-driven transformer. In *Database Systems for Advanced Applications: 27th International Conference, DASFAA 2022, Virtual Event, April 11–14, 2022, Proceedings, Part III*, pages 117–132. Springer, 2022.
- Yiming Cao, Lizhen Cui, Lei Zhang, Fuqiang Yu, Ziheng Cheng, Zhen Li, Yonghui Xu, and Chunyan Miao. Cmt: Cross-modal memory transformer for medical image report generation. In *International Conference on Database Systems for Advanced Applications*, pages 415–424. Springer, 2023.
- Joao Carreira and Andrew Zisserman. Quo vadis, action recognition? a new model and the kinetics dataset. In *proceedings of the IEEE Conference on Computer Vision and Pattern Recognition*, pages 6299–6308, 2017.
- Qingyu Chen, Yifan Peng, and Zhiyong Lu. Biosentvec: creating sentence embeddings for biomedical texts. In *2019 IEEE International Conference on Healthcare Informatics (ICHI)*, pages 1–5. IEEE, 2019.
- Weipeng Chen, Haiwei Pan, Kejia Zhang, Xin Du, and Qianna Cui. Vmeknet: Visual memory and external knowledge based network for medical report generation. In *PRICAI 2022: Trends in Artificial Intelligence: 19th Pacific Rim International Conference on Artificial Intelligence, PRICAI 2022, Shanghai, China, November 10–13, 2022, Proceedings, Part I*, pages 188–201. Springer, 2022.
- Zhihong Chen, Yan Song, Tsung-Hui Chang, and Xiang Wan. Generating radiology reports via memory-driven transformer. In *Proceedings of the 2020 Conference on Empirical Methods in Natural Language Processing (EMNLP)*, pages 1439–1449, 2020.
- Zhihong Chen, Yaling Shen, Yan Song, and Xiang Wan. Cross-modal memory networks for radiology report generation. In *Proceedings of the 59th Annual Meeting of the Association for Computational Linguistics and the 11th International Joint Conference on Natural Language Processing (Volume 1: Long Papers)*, pages 5904–5914, 2021.
- Aakanksha Chowdhery, Sharan Narang, Jacob Devlin, Maarten Bosma, Gaurav Mishra, Adam Roberts, Paul Barham, Hyung Won Chung, Charles Sutton, Sebastian Gehrmann, et al. Palm: Scaling language modeling with pathways. *Journal of Machine Learning Research*, 24(240):1–113, 2023.
- Marcella Cornia, Matteo Stefanini, Lorenzo Baraldi, and Rita Cucchiara. Meshed-memory transformer for image captioning. In *Proceedings of the IEEE/CVF conference on computer vision and pattern recognition*, pages 10578–10587, 2020.
- Francesco Dalla Serra, William Clackett, Hamish MacKinnon, Chaoyang Wang, Fani Deligianni, Jeff Dalton, and Alison Q O’Neil. Multimodal generation of radiology reports using knowledge-grounded extraction of entities and relations. In *Proceedings of the 2nd Conference of the Asia-Pacific Chapter of the Association for Computational Linguistics and the 12th International Joint Conference on Natural Language Processing*, pages 615–624, 2022.
- Francesco Dalla Serra, Chaoyang Wang, Fani Deligianni, Jeff Dalton, and Alison Q O’Neil. Controllable chest x-ray report generation from longitudinal representations. In *The 2023 Conference on Empirical Methods in Natural Language Processing*, 2023a.
- Francesco Dalla Serra, Chaoyang Wang, Fani Deligianni, Jeffrey Dalton, and Alison Q O’Neil. Finding-aware anatomical tokens for chest x-ray automated reporting. In *International Workshop on Machine Learning in Medical Imaging*, pages 413–423. Springer, 2023b.
- Dina Demner-Fushman, Marc D Kohli, Marc B Rosenman, Sonya E Shooshan, Laritza Rodriguez, Sameer Antani, George R Thoma, and Clement J McDonald. Preparing a collection of radiology examinations for distribution and retrieval. *Journal of the American Medical Informatics Association*, 23(2):304–310, 2016.
- Xin Du, Haiwei Pan, Kejia Zhang, Shuning He, Xiaofei Bian, and Weipeng Chen. Automatic report generation method based on multiscale feature extraction and word attention network. In *Asia-Pacific Web (APWeb) and Web-Age Information Management (WAIM) Joint International Conference on Web and Big Data*, pages 520–528. Springer, 2022.
- Mark Endo, Rayan Krishnan, Viswesh Krishna, Andrew Y Ng, and Pranav Rajpurkar. Retrieval-based chest x-ray report generation using a pre-trained contrastive language-image model. In *Machine Learning for Health*, pages 209–219. PMLR, 2021.
- Gaurav O Gajbhiye, Abhijeet V Nandedkar, and Ibrahima Faye. Translating medical image to radiological report: Adaptive multilevel multi-attention approach. *Computer Methods and Programs in Biomedicine*, 221:106853, 2022.
- Tiancheng Gu, Dongnan Liu, Zhiyuan Li, and Weidong Cai. Complex organ mask guided radiology report generation. In *Proceedings of the IEEE/CVF Winter Conference on Applications of Computer Vision*, pages 7995–8004, 2024.
- Zhongyi Han, Benzhen Wei, Xiaoming Xi, Bo Chen, Yilong Yin, and Shuo Li. Unifying neural learning and symbolic reasoning for spinal medical report generation. *Medical image analysis*, 67:101872, 2021.
- Kaiming He, Xiangyu Zhang, Shaoqing Ren, and Jian Sun. Deep residual learning for image recognition. In *Proceedings of the IEEE conference on computer vision and pattern recognition*, pages 770–778, 2016.
- Kaiming He, Haoqi Fan, Yuxin Wu, Saining Xie, and Ross Girshick. Momentum contrast for unsupervised visual representation learning. In *Proceedings of the IEEE/CVF conference on computer vision and pattern recognition*, pages 9729–9738, 2020.

- Sepp Hochreiter and Jürgen Schmidhuber. Long short-term memory. *Neural computation*, 9(8):1735–1780, 1997.
- Yi Hong and Charles E Kahn. Content analysis of reporting templates and free-text radiology reports. *Journal of digital imaging*, 26: 843–849, 2013.
- Benjamin Hou, Georgios Kaissis, Ronald M Summers, and Bernhard Kainz. Ratchet: Medical transformer for chest x-ray diagnosis and reporting. In *Medical Image Computing and Computer Assisted Intervention–MICCAI 2021: 24th International Conference, Strasbourg, France, September 27–October 1, 2021, Proceedings, Part VII 24*, pages 293–303. Springer, 2021a.
- Daibing Hou, Zijian Zhao, Yuying Liu, Faliang Chang, and Sanyuan Hu. Automatic report generation for chest x-ray images via adversarial reinforcement learning. *IEEE Access*, 9:21236–21250, 2021b.
- Gao Huang, Zhuang Liu, Laurens Van Der Maaten, and Kilian Q Weinberger. Densely connected convolutional networks. In *Proceedings of the IEEE conference on computer vision and pattern recognition*, pages 4700–4708, 2017.
- Jia-Hong Huang, Ting-Wei Wu, Chao-Han Huck Yang, and Marcel Worring. Deep context-encoding network for retinal image captioning. In *2021 IEEE International Conference on Image Processing (ICIP)*, pages 3762–3766. IEEE, 2021a.
- Jia-Hong Huang, C-H Huck Yang, Fangyu Liu, Meng Tian, Yi-Chieh Liu, Ting-Wei Wu, I Lin, Kang Wang, Hiromasa Morikawa, Hernghua Chang, et al. Deepopht: medical report generation for retinal images via deep models and visual explanation. In *Proceedings of the IEEE/CVF winter conference on applications of computer vision*, pages 2442–2452, 2021b.
- Jia-Hong Huang, Ting-Wei Wu, C-H Huck Yang, Zenglin Shi, I Lin, Jesper Tegner, Marcel Worring, et al. Non-local attention improves description generation for retinal images. In *Proceedings of the IEEE/CVF winter conference on applications of computer vision*, pages 1606–1615, 2022.
- Zhongzhen Huang, Xiaofan Zhang, and Shaoting Zhang. Kiut: Knowledge-injected u-transformer for radiology report generation. In *Proceedings of the IEEE/CVF Conference on Computer Vision and Pattern Recognition*, pages 19809–19818, 2023.
- Jeremy Irvin, Pranav Rajpurkar, Michael Ko, Yifan Yu, Silvana Ciurea-Ilcus, Chris Chute, Henrik Marklund, Behzad Haghgoo, Robyn Ball, Katie Shpanskaya, et al. Chexpert: A large chest radiograph dataset with uncertainty labels and expert comparison. In *Proceedings of the AAAI conference on artificial intelligence*, volume 33, pages 590–597, 2019.
- Saahil Jain, Ashwin Agrawal, Adriel Saporta, Steven QH Truong, Du Nguyen Duong, Tan Bui, Pierre Chambon, Yuhao Zhang, Matthew P Lungren, Andrew Y Ng, et al. Radgraph: Extracting clinical entities and relations from radiology reports. *arXiv preprint arXiv:2106.14463*, 2021.
- Jaehwan Jeong, Katherine Tian, Andrew Li, Sina Hartung, Subathra Adithan, Fardad Behzadi, Juan Calle, David Osayande, Michael Pohlen, and Pranav Rajpurkar. Multimodal image-text matching improves retrieval-based chest x-ray report generation. In *Medical Imaging with Deep Learning*, pages 978–990. PMLR, 2024.
- Xing Jia, Yun Xiong, Jiawei Zhang, Yao Zhang, Blackley Suzanne, Yangyong Zhu, and Chunlei Tang. Radiology report generation for rare diseases via few-shot transformer. In *IEEE International Conference on Bioinformatics and Biomedicine (BIBM)*, pages 1347–1352. IEEE, 2021.
- Xing Jia, Yun Xiong, Jiawei Zhang, Yao Zhang, Yangyong Zhu, and S Yu Philip. Few-shot radiology report generation via knowledge transfer and multi-modal alignment. In *2022 IEEE International Conference on Bioinformatics and Biomedicine (BIBM)*, pages 1574–1579. IEEE, 2022.
- Haibo Jin, Haoxuan Che, Yi Lin, and Hao Chen. Promptmrg: Diagnosis-driven prompts for medical report generation. In *Proceedings of the AAAI Conference on Artificial Intelligence*, volume 38, pages 2607–2615, 2024.
- Alistair EW Johnson, Tom J Pollard, Seth J Berkowitz, Nathaniel R Greenbaum, Matthew P Lungren, Chih-ying Deng, Roger G Mark, and Steven Horng. Mimic-cxr, a de-identified publicly available database of chest radiographs with free-text reports. *Scientific data*, 6 (1):317, 2019a.
- Alistair EW Johnson, Tom J Pollard, Nathaniel R Greenbaum, Matthew P Lungren, Chih-ying Deng, Yifan Peng, Zhiyong Lu, Roger G Mark, Seth J Berkowitz, and Steven Horng. Mimic-cxr-jpg, a large publicly available database of labeled chest radiographs. *arXiv preprint arXiv:1901.07042*, 2019b.
- Navdeep Kaur and Ajay Mittal. Radiobert: A deep learning-based system for medical report generation from chest x-ray images using contextual embeddings. *Journal of Biomedical Informatics*, 135:104220, 2022a.
- Navdeep Kaur and Ajay Mittal. Cadxreport: Chest x-ray report generation using co-attention mechanism and reinforcement learning. *Computers in Biology and Medicine*, 145:105498, 2022b.
- Navdeep Kaur, Ajay Mittal, and Gurpreem Singh. Methods for automatic generation of radiological reports of chest radiographs: a comprehensive survey. *Multimedia Tools and Applications*, 81(10):13409–13439, 2022.
- Diederik P Kingma and Max Welling. Auto-encoding variational bayes. *arXiv preprint arXiv:1312.6114*, 2013.

- Ming Kong, Zhengxing Huang, Kun Kuang, Qiang Zhu, and Fei Wu. Transq: Transformer-based semantic query for medical report generation. In *Medical Image Computing and Computer Assisted Intervention–MICCAI 2022: 25th International Conference, Singapore, September 18–22, 2022, Proceedings, Part VIII*, pages 610–620. Springer, 2022.
- Curtis P Langlotz. Radlex: a new method for indexing online educational materials, 2006.
- Jason J Lau, Soumya Gayen, Asma Ben Abacha, and Dina Demner-Fushman. A dataset of clinically generated visual questions and answers about radiology images. *Scientific data*, 5(1):1–10, 2018.
- Hojun Lee, Hyunjun Cho, Jieun Park, Jinyeong Chae, and Jihie Kim. Cross encoder-decoder transformer with global-local visual extractor for medical image captioning. *Sensors*, 22(4):1429, 2022.
- Jinhyuk Lee, Wonjin Yoon, Sungdong Kim, Donghyeon Kim, Sunkyu Kim, Chan Ho So, and Jaewoo Kang. Biobert: a pre-trained biomedical language representation model for biomedical text mining. *Bioinformatics*, 36(4):1234–1240, 2020.
- Chunyu Li, Cliff Wong, Sheng Zhang, Naoto Usuyama, Haotian Liu, Jianwei Yang, Tristan Naumann, Hoifung Poon, and Jianfeng Gao. Llava-med: Training a large language-and-vision assistant for biomedicine in one day. *Advances in Neural Information Processing Systems*, 36, 2024.
- Jun Li, Shibo Li, Ying Hu, and Hui Ren Tao. A self-guided framework for radiology report generation. In *Medical Image Computing and Computer Assisted Intervention–MICCAI 2022: 25th International Conference, Singapore, September 18–22, 2022, Proceedings, Part VIII*, pages 588–598. Springer, 2022a.
- Mingjie Li, Fuyu Wang, Xiaojun Chang, and Xiaodan Liang. Auxiliary signal-guided knowledge encoder-decoder for medical report generation. *arXiv preprint arXiv:2006.03744*, 2020.
- Mingjie Li, Wenjia Cai, Rui Liu, Yuetian Weng, Xiaoyun Zhao, Cong Wang, Xin Chen, Zhong Liu, Caineng Pan, Mengke Li, et al. Ffa-ir: Towards an explainable and reliable medical report generation benchmark. In *Thirty-fifth Conference on Neural Information Processing Systems Datasets and Benchmarks Track (Round 2)*, 2021.
- Mingjie Li, Wenjia Cai, Karin Verspoor, Shirui Pan, Xiaodan Liang, and Xiaojun Chang. Cross-modal clinical graph transformer for ophthalmic report generation. In *Proceedings of the IEEE/CVF Conference on Computer Vision and Pattern Recognition*, pages 20656–20665, 2022b.
- Mingjie Li, Bingqian Lin, Zicong Chen, Haokun Lin, Xiaodan Liang, and Xiaojun Chang. Dynamic graph enhanced contrastive learning for chest x-ray report generation. In *Proceedings of the IEEE/CVF Conference on Computer Vision and Pattern Recognition*, pages 3334–3343, 2023a.
- Mingjie Li, Rui Liu, Fuyu Wang, Xiaojun Chang, and Xiaodan Liang. Auxiliary signal-guided knowledge encoder-decoder for medical report generation. *World Wide Web*, 26(1):253–270, 2023b.
- Qingqiu Li, Jilan Xu, Runtian Yuan, Mohan Chen, Yuejie Zhang, Rui Feng, Xiaobo Zhang, and Shang Gao. Enhanced knowledge injection for radiology report generation. In *2023 IEEE International Conference on Bioinformatics and Biomedicine (BIBM)*, pages 2053–2058. IEEE, 2023c.
- Yaowei Li, Bang Yang, Xuxin Cheng, Zhihong Zhu, Hongxiang Li, and Yuexian Zou. Unify, align and refine: Multi-level semantic alignment for radiology report generation. In *Proceedings of the IEEE/CVF International Conference on Computer Vision*, pages 2863–2874, 2023d.
- Yuxiang Liao, Hantao Liu, and Irena Spasić. Deep learning approaches to automatic radiology report generation: A systematic review. *Informatics in Medicine Unlocked*, page 101273, 2023.
- Chin-Yew Lin. Rouge: A package for automatic evaluation of summaries. In *Text summarization branches out*, pages 74–81, 2004.
- Zhihong Lin, Donghao Zhang, Danli Shi, Renjing Xu, Qingyi Tao, Lin Wu, Mingguang He, and Zongyuan Ge. Contrastive pre-training and linear interaction attention-based transformer for universal medical reports generation. *Journal of Biomedical Informatics*, page 104281, 2023.
- Chang Liu, Yuanhe Tian, and Yan Song. A systematic review of deep learning-based research on radiology report generation. *arXiv preprint arXiv:2311.14199*, 2023a.
- Fenglin Liu, Shen Ge, and Xian Wu. Competence-based multimodal curriculum learning for medical report generation. In *Proceedings of the 59th Annual Meeting of the Association for Computational Linguistics and the 11th International Joint Conference on Natural Language Processing (Volume 1: Long Papers)*, pages 3001–3012, 2021a.
- Fenglin Liu, Xian Wu, Shen Ge, Wei Fan, and Yuexian Zou. Exploring and distilling posterior and prior knowledge for radiology report generation. In *Proceedings of the IEEE/CVF conference on computer vision and pattern recognition*, pages 13753–13762, 2021b.
- Fenglin Liu, Changchang Yin, Xian Wu, Shen Ge, Ping Zhang, and Xu Sun. Contrastive attention for automatic chest x-ray report generation. In *Findings of the Association for Computational Linguistics: ACL-IJCNLP*, page 269–280, 2021c.
- Fenglin Liu, Chenyu You, Xian Wu, Shen Ge, Xu Sun, et al. Auto-encoding knowledge graph for unsupervised medical report generation. *Advances in Neural Information Processing Systems*, 34:16266–16279, 2021d.

- Guangyi Liu, Yinghong Liao, Fuyu Wang, Bin Zhang, Lu Zhang, Xiaodan Liang, Xiang Wan, Shaolin Li, Zhen Li, Shuixing Zhang, et al. Medical-vlbert: Medical visual language bert for covid-19 ct report generation with alternate learning. *IEEE Transactions on Neural Networks and Learning Systems*, 32(9):3786–3797, 2021e.
- Guanxiong Liu, Tzu-Ming Harry Hsu, Matthew McDermott, Willie Boag, Wei-Hung Weng, Peter Szolovits, and Marzyeh Ghassemi. Clinically accurate chest x-ray report generation. In *Machine Learning for Healthcare Conference*, pages 249–269. PMLR, 2019.
- Zhizhe Liu, Zhenfeng Zhu, Shuai Zheng, Yawei Zhao, Kunlun He, and Yao Zhao. From observation to concept: A flexible multi-view paradigm for medical report generation. *IEEE Transactions on Multimedia*, 2023b.
- Pablo Messina, Pablo Pino, Denis Parra, Alvaro Soto, Cecilia Besa, Sergio Uribe, Marcelo Andía, Cristian Tejos, Claudia Prieto, and Daniel Capurro. A survey on deep learning and explainability for automatic report generation from medical images. *ACM Computing Surveys (CSUR)*, 54(10s):1–40, 2022.
- Zahra Mirikharaji, Kumar Abhishek, Alceu Bissoto, Catarina Barata, Sandra Avila, Eduardo Valle, M Emre Celebi, and Ghassan Hamarneh. A survey on deep learning for skin lesion segmentation. *Medical Image Analysis*, page 102863, 2023.
- Yasuhide Miura, Yuhao Zhang, Emily Tsai, Curtis Langlotz, and Dan Jurafsky. Improving factual completeness and consistency of image-to-text radiology report generation. In *Proceedings of the 2021 Conference of the North American Chapter of the Association for Computational Linguistics: Human Language Technologies*, pages 5288–5304, 2021.
- Mashood Mohammad Mohsan, Muhammad Usman Akram, Ghulam Rasool, Norah Saleh Alghamdi, Muhammad Abdullah Aamer Baqai, and Muhammad Abbas. Vision transformer and language model based radiology report generation. *IEEE Access*, 11:1814–1824, 2022.
- Jong Hak Moon, Hyungyung Lee, Woncheol Shin, Young-Hak Kim, and Edward Choi. Multi-modal understanding and generation for medical images and text via vision-language pre-training. *IEEE Journal of Biomedical and Health Informatics*, 26(12):6070–6080, 2022.
- Ivona Najdenkoska, Xiantong Zhen, Marcel Worring, and Ling Shao. Variational topic inference for chest x-ray report generation. In *Medical Image Computing and Computer Assisted Intervention—MICCAI 2021: 24th International Conference, Strasbourg, France, September 27–October 1, 2021, Proceedings, Part III 24*, pages 625–635. Springer, 2021.
- Ivona Najdenkoska, Xiantong Zhen, Marcel Worring, and Ling Shao. Uncertainty-aware report generation for chest x-rays by variational topic inference. *Medical Image Analysis*, 82:102603, 2022.
- J Martijn Nobel, Koos van Geel, and Simon GF Robben. Structured reporting in radiology: a systematic review to explore its potential. *European radiology*, pages 1–18, 2022.
- OpenAI. Chatgpt: Optimizing language models for dialogue. 2023. URL <https://openai.com/blog/chatgpt/>.
- Esha Pahwa, Dwij Mehta, Sanjeet Kapadia, Devansh Jain, and Achleshwar Luthra. Medskip: Medical report generation using skip connections and integrated attention. In *Proceedings of the IEEE/CVF International Conference on Computer Vision*, pages 3409–3415, 2021.
- Abhineet Pandey, Bhawna Paliwal, Abhinav Dhall, Ramanathan Subramanian, and Dwarikanath Mahapatra. This explains that: Congruent image–report generation for explainable medical image analysis with cyclic generative adversarial networks. In *Interpretability of Machine Intelligence in Medical Image Computing, and Topological Data Analysis and Its Applications for Medical Data: 4th International Workshop, iMIMIC 2021, and 1st International Workshop, TDA4MedicalData 2021, Held in Conjunction with MICCAI 2021, Strasbourg, France, September 27, 2021, Proceedings 4*, pages 34–43. Springer, 2021.
- Kishore Papineni, Salim Roukos, Todd Ward, and Wei-Jing Zhu. Bleu: a method for automatic evaluation of machine translation. In *Proceedings of the 40th annual meeting of the Association for Computational Linguistics*, pages 311–318, 2002.
- Chantal Pellegrini, Matthias Keicher, Ege Özsoy, and Nassir Navab. Rad-restruct: A novel vqa benchmark and method for structured radiology reporting. In *International Conference on Medical Image Computing and Computer-Assisted Intervention*, pages 409–419. Springer, 2023.
- Pablo Pino, Denis Parra, Cecilia Besa, and Claudio Lagos. Clinically correct report generation from chest x-rays using templates. In *Machine Learning in Medical Imaging: 12th International Workshop, MLMI 2021, Held in Conjunction with MICCAI 2021, Strasbourg, France, September 27, 2021, Proceedings 12*, pages 654–663. Springer, 2021.
- Emmanouil Antonios Platanios, Otilia Stretcu, Graham Neubig, Barnabás Póczós, and Tom Mitchell. Competence-based curriculum learning for neural machine translation. In *Proceedings of the 2019 Conference of the North American Chapter of the Association for Computational Linguistics: Human Language Technologies, Volume 1 (Long and Short Papers)*, pages 1162–1172, 2019.
- Han Qin and Yan Song. Reinforced cross-modal alignment for radiology report generation. In *Findings of the Association for Computational Linguistics: ACL 2022*, pages 448–458, 2022.
- Alec Radford, Jong Wook Kim, Chris Hallacy, Aditya Ramesh, Gabriel Goh, Sandhini Agarwal, Girish Sastry, Amanda Askell, Pamela Mishkin, Jack Clark, et al. Learning transferable visual models from natural language supervision. In *International conference on machine learning*, pages 8748–8763. PMLR, 2021.

- Aditya Ramesh, Mikhail Pavlov, Gabriel Goh, Scott Gray, Chelsea Voss, Alec Radford, Mark Chen, and Ilya Sutskever. Zero-shot text-to-image generation. In *International conference on machine learning*, pages 8821–8831. Pmlr, 2021.
- Vignav Ramesh, Nathan A Chi, and Pranav Rajpurkar. Improving radiology report generation systems by removing hallucinated references to non-existent priors. In *Machine Learning for Health*, pages 456–473. PMLR, 2022.
- Shaoqing Ren, Kaiming He, Ross Girshick, and Jian Sun. Faster r-cnn: Towards real-time object detection with region proposal networks. *Advances in neural information processing systems*, 28, 2015.
- Khaled Saab, Tao Tu, Wei-Hung Weng, Ryutaro Tanno, David Stutz, Ellery Wulczyn, Fan Zhang, Tim Strother, Chunjong Park, Elahe Vedadi, et al. Capabilities of gemini models in medicine. *arXiv preprint arXiv:2404.18416*, 2024.
- Alexander Selivanov, Oleg Y Rogov, Daniil Chesakov, Artem Shelmanov, Irina Fedulova, and Dmitry V Dylov. Medical image captioning via generative pretrained transformers. *Scientific Reports*, 13(1):4171, 2023.
- Fahad Shamshad, Salman Khan, Syed Waqas Zamir, Muhammad Haris Khan, Munawar Hayat, Fahad Shahbaz Khan, and Huazhu Fu. Transformers in medical imaging: A survey. *Medical Image Analysis*, page 102802, 2023.
- Shashank Shetty, Ananthanarayana VS, and Ajit Mahale. Cross-modal deep learning-based clinical recommendation system for radiology report generation from chest x-rays. *International Journal of Engineering*, 2023.
- Karen Simonyan and Andrew Zisserman. Very deep convolutional networks for large-scale image recognition. *arXiv preprint arXiv:1409.1556*, 2014.
- Sonit Singh, Sarvnaz Karimi, Kevin Ho-Shon, and Len Hamey. Show, tell and summarise: learning to generate and summarise radiology findings from medical images. *Neural Computing and Applications*, 33:7441–7465, 2021.
- Karan Singhal, Tao Tu, Juraj Gottweis, Rory Sayres, Ellery Wulczyn, Le Hou, Kevin Clark, Stephen Pfohl, Heather Cole-Lewis, Darlene Neal, et al. Towards expert-level medical question answering with large language models. *arXiv preprint arXiv:2305.09617*, 2023.
- Mehreen Sirshar, Muhammad Faheem Khalil Paracha, Muhammad Usman Akram, Norah Saleh Alghamdi, Syeda Zainab Yousuf Zaidi, and Tatheer Fatima. Attention based automated radiology report generation using cnn and lstm. *Plos one*, 17(1):e0262209, 2022.
- Akshay Smit, Saahil Jain, Pranav Rajpurkar, Anuj Pareek, Andrew Y Ng, and Matthew Lungren. Combining automatic labelers and expert annotations for accurate radiology report labeling using bert. In *Proceedings of the 2020 Conference on Empirical Methods in Natural Language Processing (EMNLP)*, pages 1500–1519, 2020.
- Xiao Song, Xiaodan Zhang, Junzhong Ji, Ying Liu, and Pengxu Wei. Cross-modal contrastive attention model for medical report generation. In *Proceedings of the 29th International Conference on Computational Linguistics*, pages 2388–2397, 2022.
- Statistics. Diagnostic imaging dataset., 2020. URL <https://www.england.nhs.uk/statistics/statistical-work-areas/diagnostic-imaging-dataset/>.
- Jinghan Sun, Dong Wei, Liansheng Wang, and Yefeng Zheng. Lesion guided explainable few weak-shot medical report generation. In *Medical Image Computing and Computer Assisted Intervention–MICCAI 2022: 25th International Conference, Singapore, September 18–22, 2022, Proceedings, Part V*, pages 615–625. Springer, 2022.
- Ke Sun, Bin Xiao, Dong Liu, and Jingdong Wang. Deep high-resolution representation learning for human pose estimation. In *Proceedings of the IEEE/CVF conference on computer vision and pattern recognition*, pages 5693–5703, 2019a.
- Zhaoyi Sun, Hanley Ong, Patrick Kennedy, Liyan Tang, Shirley Chen, Jonathan Elias, Eugene Lucas, George Shih, and Yifan Peng. Evaluating gpt-4 on impressions generation in radiology reports. *Radiology*, 307(5):e231259, 2023.
- Zhiqing Sun, Zhi-Hong Deng, Jian-Yun Nie, and Jian Tang. Rotate: Knowledge graph embedding by relational rotation in complex space. *arXiv preprint arXiv:1902.10197*, 2019b.
- Christian Szegedy, Vincent Vanhoucke, Sergey Ioffe, Jon Shlens, and Zbigniew Wojna. Rethinking the inception architecture for computer vision. In *Proceedings of the IEEE conference on computer vision and pattern recognition*, pages 2818–2826, 2016.
- Mingxing Tan and Quoc Le. Efficientnet: Rethinking model scaling for convolutional neural networks. In *International conference on machine learning*, pages 6105–6114. PMLR, 2019.
- Tim Tanida, Philip Müller, Georgios Kaissis, and Daniel Rueckert. Interactive and explainable region-guided radiology report generation. In *Proceedings of the IEEE/CVF Conference on Computer Vision and Pattern Recognition*, pages 7433–7442, 2023.
- Ajay K Tanwani, Joelle Barral, and Daniel Freedman. Reptsnet: Combining vision with language for automated medical reports. In *Medical Image Computing and Computer Assisted Intervention–MICCAI 2022: 25th International Conference, Singapore, September 18–22, 2022, Proceedings, Part V*, pages 714–724. Springer, 2022.
- Gemini Team, Rohan Anil, Sebastian Borgeaud, Yonghui Wu, Jean-Baptiste Alayrac, Jiahui Yu, Radu Soricut, Johan Schalkwyk, Andrew M Dai, Anja Hauth, et al. Gemini: a family of highly capable multimodal models. *arXiv preprint arXiv:2312.11805*, 2023.
- Eric Topol. *Deep medicine: how artificial intelligence can make healthcare human again*. Hachette UK, 2019.

- Tao Tu, Shekoofeh Azizi, Danny Driess, Mike Schaeckermann, Mohamed Amin, Pi-Chuan Chang, Andrew Carroll, Charles Lau, Ryutaro Tanno, Ira Ktena, et al. Towards generalist biomedical ai. *NEJM AI*, 1(3):AIoa2300138, 2024.
- Emiel Van Miltenburg, Desmond Elliott, and Piek Vossen. Measuring the diversity of automatic image descriptions. In *Proceedings of the 27th International Conference on Computational Linguistics*, pages 1730–1741, 2018.
- Ashish Vaswani, Noam Shazeer, Niki Parmar, Jakob Uszkoreit, Llion Jones, Aidan N Gomez, Łukasz Kaiser, and Illia Polosukhin. Attention is all you need. *Advances in neural information processing systems*, 30, 2017.
- Ramakrishna Vedantam, C Lawrence Zitnick, and Devi Parikh. Cider: Consensus-based image description evaluation. In *Proceedings of the IEEE conference on computer vision and pattern recognition*, pages 4566–4575, 2015.
- Jun Wang, Abhir Bhalerao, and Yulan He. Cross-modal prototype driven network for radiology report generation. In *Computer Vision—ECCV 2022: 17th European Conference, Tel Aviv, Israel, October 23–27, 2022, Proceedings, Part XXXV*, pages 563–579. Springer, 2022a.
- Jun Wang, Abhir Bhalerao, Terry Yin, Simon See, and Yulan He. Camanet: class activation map guided attention network for radiology report generation. *IEEE Journal of Biomedical and Health Informatics*, 2024a.
- Lin Wang, Munan Ning, Donghuan Lu, Dong Wei, Yefeng Zheng, and Jie Chen. An inclusive task-aware framework for radiology report generation. In *Medical Image Computing and Computer Assisted Intervention—MICCAI 2022: 25th International Conference, Singapore, September 18–22, 2022, Proceedings, Part VIII*, pages 568–577. Springer, 2022b.
- Sheng Wang, Zihao Zhao, Xi Ouyang, Qian Wang, and Dinggang Shen. Chatcad: Interactive computer-aided diagnosis on medical image using large language models. *arXiv preprint arXiv:2302.07257*, 2023a.
- Siyuan Wang, Bo Peng, Yichao Liu, and Qi Peng. Fine-grained medical vision-language representation learning for radiology report generation. In *Proceedings of the 2023 Conference on Empirical Methods in Natural Language Processing*, pages 15949–15956, 2023b.
- Song Wang, Liyan Tang, Mingquan Lin, George Shih, Ying Ding, and Yifan Peng. Prior knowledge enhances radiology report generation. In *AMIA Annual Symposium Proceedings*, volume 2022, page 486. American Medical Informatics Association, 2022c.
- Yixin Wang, Zihao Lin, Zhe Xu, Haoyu Dong, Jie Luo, Jiang Tian, Zhongchao Shi, Lifu Huang, Yang Zhang, Jianping Fan, et al. Trust it or not: Confidence-guided automatic radiology report generation. *Neurocomputing*, page 127374, 2024b.
- Yuhao Wang, Kai Wang, Xiaohong Liu, Tianrun Gao, Jingyue Zhang, and Guangyu Wang. Self adaptive global-local feature enhancement for radiology report generation. In *2023 IEEE International Conference on Image Processing (ICIP)*, pages 2275–2279. IEEE, 2023c.
- Zhanyu Wang, Luping Zhou, Lei Wang, and Xiu Li. A self-boosting framework for automated radiographic report generation. In *Proceedings of the IEEE/CVF Conference on Computer Vision and Pattern Recognition*, pages 2433–2442, 2021.
- Zhanyu Wang, Hongwei Han, Lei Wang, Xiu Li, and Luping Zhou. Automated radiographic report generation purely on transformer: A multicriteria supervised approach. *IEEE Transactions on Medical Imaging*, 41(10):2803–2813, 2022d.
- Zhanyu Wang, Mingkang Tang, Lei Wang, Xiu Li, and Luping Zhou. A medical semantic-assisted transformer for radiographic report generation. In *Medical Image Computing and Computer Assisted Intervention—MICCAI 2022: 25th International Conference, Singapore, September 18–22, 2022, Proceedings, Part III*, pages 655–664. Springer, 2022e.
- Zhanyu Wang, Lingqiao Liu, Lei Wang, and Luping Zhou. Metransformer: Radiology report generation by transformer with multiple learnable expert tokens. In *Proceedings of the IEEE/CVF Conference on Computer Vision and Pattern Recognition*, pages 11558–11567, 2023d.
- Joy Wu, Nkechinyere Agu, Ismini Lourentzou, Arjun Sharma, Joseph Paguio, Jasper Seth Yao, Edward Christopher Dee, William Mitchell, Satyananda Kashyap, Andrea Giovannini, et al. Chest imagenome dataset. *Physio Net*, 2021.
- Xing Wu, Jingwen Li, Jianjia Wang, and Quan Qian. Multimodal contrastive learning for radiology report generation. *Journal of Ambient Intelligence and Humanized Computing*, pages 1–10, 2022.
- Yuexin Wu, I-Chan Huang, and Xiaolei Huang. Token imbalance adaptation for radiology report generation. In *Conference on Health, Inference, and Learning*, pages 72–85. PMLR, 2023.
- Saining Xie, Ross Girshick, Piotr Dollár, Zhuowen Tu, and Kaiming He. Aggregated residual transformations for deep neural networks. In *Proceedings of the IEEE conference on computer vision and pattern recognition*, pages 1492–1500, 2017.
- Chen Xu, Bojie Hu, Yufan Jiang, Kai Feng, Zeyang Wang, Shen Huang, Qi Ju, Tong Xiao, and Jingbo Zhu. Dynamic curriculum learning for low-resource neural machine translation. In *Proceedings of the 28th International Conference on Computational Linguistics*, pages 3977–3989, 2020.
- Dexuan Xu, Huashi Zhu, Yu Huang, Zhi Jin, Weiping Ding, Hang Li, and Menglong Ran. Vision-knowledge fusion model for multi-domain medical report generation. *Information Fusion*, 97:101817, 2023.
- Youyuan Xue, Yun Tan, Ling Tan, Jiaohua Qin, and Xuyu Xiang. Generating radiology reports via auxiliary signal guidance and a memory-driven network. *Expert Systems with Applications*, 237:121260, 2024.

- Bin Yan, Mingtao Pei, Meng Zhao, Caifeng Shan, and Zhaoxing Tian. Prior guided transformer for accurate radiology reports generation. *IEEE Journal of Biomedical and Health Informatics*, 26(11):5631–5640, 2022.
- Sixing Yan. Memory-aligned knowledge graph for clinically accurate radiology image report generation. In *Proceedings of the 21st Workshop on Biomedical Language Processing*, pages 116–122, 2022.
- Zhiling Yan, Kai Zhang, Rong Zhou, Lifang He, Xiang Li, and Lichao Sun. Multimodal chatgpt for medical applications: an experimental study of gpt-4v. *arXiv preprint arXiv:2310.19061*, 2023.
- Shaokang Yang, Jianwei Niu, Jiyan Wu, Yong Wang, Xuefeng Liu, and Qingfeng Li. Automatic ultrasound image report generation with adaptive multimodal attention mechanism. *Neurocomputing*, 427:40–49, 2021a.
- Shuxin Yang, Xian Wu, Shen Ge, S Kevin Zhou, and Li Xiao. Knowledge matters: Chest radiology report generation with general and specific knowledge. *Medical Image Analysis*, 80:102510, 2022.
- Shuxin Yang, Xian Wu, Shen Ge, Zhuozhao Zheng, S Kevin Zhou, and Li Xiao. Radiology report generation with a learned knowledge base and multi-modal alignment. *Medical Image Analysis*, 86:102798, 2023.
- Yan Yang, Jun Yu, Jian Zhang, Weidong Han, Hanliang Jiang, and Qingming Huang. Joint embedding of deep visual and semantic features for medical image report generation. *IEEE Transactions on Multimedia*, 2021b.
- Di You, Fenglin Liu, Shen Ge, Xiaoxia Xie, Jing Zhang, and Xian Wu. Aligntransformer: Hierarchical alignment of visual regions and disease tags for medical report generation. In *Medical Image Computing and Computer Assisted Intervention—MICCAI 2021: 24th International Conference, Strasbourg, France, September 27–October 1, 2021, Proceedings, Part III 24*, pages 72–82. Springer, 2021.
- Jingyi You, Dongyuan Li, Manabu Okumura, and Kenji Suzuki. Jpg-jointly learn to align: Automated disease prediction and radiology report generation. In *Proceedings of the 29th International Conference on Computational Linguistics*, pages 5989–6001, 2022.
- Junsan Zhang, Xiuxuan Shen, Shaohua Wan, Sotirios K Goudos, Jie Wu, Ming Cheng, and Weishan Zhang. A novel deep learning model for medical report generation by inter-intra information calibration. *IEEE Journal of Biomedical and Health Informatics*, 2023a.
- Ke Zhang, Hanliang Jiang, Jian Zhang, Qingming Huang, Jianping Fan, Jun Yu, and Weidong Han. Semi-supervised medical report generation via graph-guided hybrid feature consistency. *IEEE Transactions on Multimedia*, 2023b.
- Yixiao Zhang, Xiaosong Wang, Ziyue Xu, Qihang Yu, Alan Yuille, and Daguang Xu. When radiology report generation meets knowledge graph. In *Proceedings of the AAAI Conference on Artificial Intelligence*, volume 34, pages 12910–12917, 2020.
- Yong Zhang, Weihua Ou, Jiacheng Zhang, and Jiabin Deng. Category supervised cross-modal hashing retrieval for chest x-ray and radiology reports. *Computers & Electrical Engineering*, 98:107673, 2022.
- Bolei Zhou, Aditya Khosla, Agata Lapedriza, Aude Oliva, and Antonio Torralba. Learning deep features for discriminative localization. In *Proceedings of the IEEE conference on computer vision and pattern recognition*, pages 2921–2929, 2016.
- Yi Zhou, Lei Huang, Tao Zhou, Huazhu Fu, and Ling Shao. Visual-textual attentive semantic consistency for medical report generation. In *Proceedings of the IEEE/CVF International Conference on Computer Vision*, pages 3985–3994, 2021.
- Jun-Yan Zhu, Taesung Park, Phillip Isola, and Alexei A Efros. Unpaired image-to-image translation using cycle-consistent adversarial networks. In *Proceedings of the IEEE international conference on computer vision*, pages 2223–2232, 2017.

Appendix A

Table A1: Summary of papers in the survey. The overview is based on the findings of the survey. The dataset and metrics section focuses on mainstream datasets and metrics. ‘-’ indicates that the paper either does not detail this process or does not include the key techniques summarized in this survey. The following abbreviations are used: I-Archi: the architecture of image feature learning, I-Module: the enhancement module of image feature learning, NI: the feature learning of non-image data, GEI: gastrointestinal endoscope image, RetiI: retinal image, Term: terminology, KnowB: knowledge base, RealR: real report, ClinicalI: clinical information, Ques: questionnaires, FreFilter: frequency-based filtering, ConAtoL: converting all tokens to lowercase, RemoNAT: removing non-alphabetic tokens, AT: auxiliary task, ConrasL: Contrastive learning, MM: memory metric, FeatO: feature-level operation, OptimS: optimization strategies, H-LSTM: hierarchical LSTM, ReLoss: re-weighted loss function, ReinL: reinforcement learning, R-L: Rouge-L, C-D: CIDER-D, CE: clinical efficacy, Com: comparison, Clas: classification, EScore: error scoring, ECI: extracting case-related information, IU: IU X-Ray, MIMIC: MIMIC-CXR, ImaGeno: Chest ImaGenome, COV: COV-CTR, DeepEye: DeepEyeNet, CCCT: Chinese COVID-19 CT, Ret-I: Retina ImBank, and Ret-C: Retina Chinese. In addition, AT-Graph, AT-Class, AT-EC, and AT-DS mean the graph-based, classification, embedding comparison, and detection/segmentation auxiliary tasks.

Paper	Input data	Data preparation	Feature Learning			Feature Fusion	Generation	Training Strategy	Datasets	Metrics
			I-Archi	I-Module	NI					
Liu et al. [2021b]	Chest X-ray, Term, RealR	Tokenizing, ConAtoL, RemoNAT, FreFilter	ResNet	AT-Graph	Transformer	FeatO	Transformer	-	IU, MIMIC	BLEU, R-L, METEOR, C-D
Liu et al. [2021d]	Chest X-ray	-	ResNet	AT-Graph	-	-	Transformer	-	IU, MIMIC	BLEU, R-L, METEOR, CE, Com
Liu et al. [2021a]	Chest X-ray	Tokenizing, ConAtoL, RemoNAT	CNNs	-	-	-	LSTMs	Curriculum learning	IU, MIMIC	BLEU, R-L, METEOR, Com
Chen et al. [2021]	Chest X-ray	-	ResNet+ Transformer	-	-	MM	Transformer	-	IU, MIMIC	BLEU, R-L, METEOR, CE
You et al. [2021]	Chest X-ray	-	ResNet	-	-	Attention	Transformer	-	IU, MIMIC	BLEU, R-L, METEOR, Com
Miura et al. [2021]	Chest X-ray	-	DenseNet+ Transformer	-	-	-	Transformer	ReinL	MIMIC	BLEU, C-D, CE, Com
Alfarghaly et al. [2021]	Chest X-ray	Resizing	DenseNet	AT-Class	-	Attention	Transformer	-	IU	BLEU, R-L, METEOR, C-D, Clas
Yang et al. [2021b]	Chest X-ray	-	ResNet	AT-EC	-	-	H-LSTM	-	IU, MIMIC	BLEU, R-L, C-D
Pahwa et al. [2021]	Chest X-ray	Resizing, Cropping, Flipping	HRNet+ Transformer	-	-	-	R2Gen	-	IU	BLEU, R-L, METEOR
Zhou et al. [2021]	Chest X-ray, ClinicalI	Tokenizing, FreFilter	DenseNet	AT-Class, AT-EC	One-hot, BioSentVec	Attention	H-LSTM	-	IU, MIMIC	BLEU, R-L, METEOR, C-D, nKTD
Huang et al. [2021b]	RetiI, Term	-	CNNs	-	Embedding layer	FeatO	LSTM	-	DeepEye	BLEU, R-L, C-D

Continued on next page

Table A1 – continued from previous page

Paper	Input data	Data preparation	Feature Learning			Feature Fusion	Generation	Training Strategy	Dataset	Metrics
			I-Archi	I-Module	NI					
Han et al. [2021]	Spine MRI	–	Self-design	AT-DS	–	–	Reasoning	–	–	–
Liu et al. [2021e]	Chest X-ray, Chest CT, Term	–	DenseNet	AT-Class	BERT	FeatO, Attention	Transformer	AT	CCCT	BLEU, R-L, C-D, Com
Wang et al. [2021]	Chest X-ray, Chest CT	Tokenizing	ResNet+ Transformer	AT-EC	–	–	H-LSTM	AT	IU, COV	BLEU, R-L, C-D
Endo et al. [2021]	Chest X-ray	–	ResNet	–	–	–	Retrieval	–	MIMIC	BLEU, S_{emb} , CE
Najdenkoska et al. [2021]	Chest X-ray	Resizing, Tokenizing, ConAtoL, RemoNAT, FreFilter	DenseNet+ Transformer	AT-EC	–	–	LSTM	–	IU, MIMIC	BLEU, R-L, METEOR, CE
Yang et al. [2021a]	Breast ultrasound	Tokenizing, FreFilter	ResNet	AT-Class	–	FeatO	LSTM	–	BCD2018	BLEU, R-L, METEOR, C-D
Pandey et al. [2021]	Chest X-ray	Resizing	VGG	–	–	–	H-LSTM	AT	IU	BLEU, R-L
Hou et al. [2021b]	Chest X-ray	Resizing, Tokenizing, FreFilter	ResNet	AT-Class	–	LSTM	H-LSTM	ReinL	IU, MIMIC	BLEU, R-L, METEOR, C-D, CE
Pino et al. [2021]	Chest X-ray	–	DenseNet	–	–	–	Template	–	IU, MIMIC	BLEU, R-L, C-D, CE, MIRQI
Liu et al. [2021c]	Chest X-ray	Tokenizing, ConAtoL, FreFilter	ResNet	ContrasL	–	–	H-LSTM	–	IU, MIMIC	BLEU, R-L, METEOR, CE, Com
Jia et al. [2021]	Chest X-ray	–	ResNet+ Transformer	–	–	–	Transformer	–	IU, MIMIC	BLEU, R-L
Hou et al. [2021a]	Chest X-ray	Resizing, Data augmentation	DenseNet	–	–	–	Transformer	–	MIMIC	BLEU, R-L, METEOR, CE
Huang et al. [2021a]	RetiI, Term	Tokenizing, ConAtoL, RemoNAT, FreFilter	CNNs	–	Embedding layer	LSTM	LSTM	–	DeepEye	BLEU, R-L, C-D
Babar et al. [2021a]	Chest X-ray	Tokenizing, ConAtoL, RemoNAT	–	–	–	–	Uncondition	–	IU, MIMIC	BLEU, R-L, METEOR, C-D, CE
Singh et al. [2021]	Chest X-ray	Resizing, Tokenizing, ConAtoL, RemoNAT, FreFilter	InceptionV3	AT-Class	–	–	LSTM	–	IU, MIMIC	BLEU, R-L, METEOR, C-D

Continued on next page

Table A1 – continued from previous page

Paper	Input data	Data preparation	Feature Learning			Feature Fusion	Generation	Training Strategy	Dataset	Metrics
			I-Archi	I-Module	NI					
Yang et al. [2022]	Chest X-ray, KnowB, RealR	Resizing, Tokenizing, ConAtoL, FreFilter	ResNet	–	RotatE, ECI, BERT	Attention	Transformer	–	IU, MIMIC	BLEU, R-L, C-D, CE
Ramesh et al. [2022]	Chest X-ray	Tokenizing, Filtering	ResNet/Transformer	–	–	–	Retrieval	–	MIMIC	S_{emb}
Sirshar et al. [2022]	Chest X-ray	Tokenizing, RemoNAT, ConAtoL	VGG	–	–	–	LSTM	–	IU, MIMIC	BLEU
Najdenkoska et al. [2022]	Chest X-ray	Resizing, RemoNAT, FreFilter	DenseNet+Transformer	AT-EC	–	–	Transformer, LSTM	–	IU, MIMIC	BLEU, R-L, METEOR, %Novel, CE
Wang et al. [2022c]	Chest X-ray	Cropping, Tokenizing, ConAtoL, FreFilter	DenseNet	AT-Graph	–	–	H-LSTM	–	IU	BLEU, R-L, C-D
Li et al. [2022b]	Retil	Resizing, Tokenizing, ConAtoL, FreFilter	I3D+Transformer	AT-Graph	–	–	Transformer	–	FFA-IR	BLEU, R-L, METEOR, C-D, Com
Qin and Song [2022]	Chest X-ray	–	ResNet+Transformer	–	–	MM	Transformer	ReinL	IU, MIMIC	BLEU, R-L, METEOR, CE, Com
Wang et al. [2022a]	Chest X-ray	Resizing, Cropping	ResNet+Transformer	ContrasL	–	MM	Transformer	–	IU, MIMIC	BLEU, R-L, METEOR, C-D
Cao et al. [2022]	Chest X-ray, GEI, Term	–	DenseNet+Transformer	AT-Graph	BERT	FeatO, Attention	Transformer	–	IU	BLEU, R-L, C-D, Com
Mohsan et al. [2022]	Chest X-ray	Tokenizing, ConAtoL	Transformer	–	–	–	Transformer	–	IU	BLEU, R-L, METEOR, C-D
Yan [2022]	Chest X-ray	–	DenseNet+Transformer	AT-Graph, MM	–	–	Transformer	–	IU, MIMIC	BLEU, R-L, METEOR, C-D, CE, MIRQI
Li et al. [2022a]	Chest X-ray	–	ResNet+Transformer	AT-Class	–	–	Transformer	AT	IU	BLEU, R-L, METEOR
Sun et al. [2022]	Retil	Resizing	ResNet+ Faster-RCNN	AT-EC, AT-DS	–	–	Transformer	–	FFA-IR	BLEU, R-L, METEOR, C-D
You et al. [2022]	Chest X-ray	Tokenizing, ConAtoL, RemoNAT	ResNet+Transformer	AT-Class	–	Attention, MM	Transformer	–	IU	BLEU, R-L, METEOR
Wang et al. [2022d]	Chest X-ray	Resizing	Transformer	AT-Class, AT-EC	–	–	Transformer	ReLoss	IU, MIMIC	BLEU, R-L, C-D

Continued on next page

Table A1 – continued from previous page

Paper	Input data	Data preparation	Feature Learning			Feature Fusion	Generation	Training Strategy	Dataset	Metrics
			I-Archi	I-Module	NI					
Lee et al. [2022]	Chest X-ray	Resizing, Cropping, Flipping	ResNet+ Transformer	–	–	–	R2Gen	–	IU	BLEU, R-L, METEOR
Moon et al. [2022]	Chest X-ray	Resizing, Cropping, Tokenizing	ResNet+ Transformer	AT	–	–	Transformer	–	IU, MIMIC	BLEU, CE
Huang et al. [2022]	Retil, Term	Resizing, Tokenizing, ConAtoL, RemoNAT, FreFilter	CNNs	–	Embedding layer	Attention	LSTM	–	DeepEye	BLEU, R-L, C-D
Kaur and Mittal [2022a]	Chest X-ray	Resizing, Convert image to grayscale, Flipping, Tokenizing, ConAtoL, RemoNAT	VGG	–	–	–	H-LSTM	–	IU	BLEU, R-L, C-D
Song et al. [2022]	Chest X-ray, RealR	–	DenseNet	ContrasL	–	Attention	Transformer	–	IU, MIMIC	BLEU, R-L, METEOR, CE
Jia et al. [2022]	Chest X-ray	–	DenseNet	–	–	Attention	H-LSTM	–	IU, MIMIC	BLEU, R-L
Zhang et al. [2022]	Chest X-ray	Resizing	VGG	–	–	–	Retrieval	–	MIMIC	Precision
Dalla Serra et al. [2022]	Chest X-ray, ClinicalI	Tokenizing, Resizing, Flipping, Rotation, Cropping	ResNet+ Transformer	AT-Graph	Embedding layer	Attention	Transformer	–	MIMIC	BLEU, R-L, METEOR, CE, Com
Yan et al. [2022]	Chest X-ray	Tokenizing, ConAtoL, FreFilter	ResNet+ Transformer	AT	–	Attention	Transformer	–	IU, MIMIC	BLEU, R-L, METEOR, C-D, CE
Gajbhiye et al. [2022]	Chest X-ray	Tokenizing, Removing irrelevant elements, ConAtoL, FreFilter	DenseNet	AT-Class	–	–	LSTM	ReLoss	IU	BLEU, R-L, METEOR, C-D
Wang et al. [2022b]	Chest X-ray	Grouping	ResNet+ Transformer	AT-Class	–	–	R2Gen	–	IU, MIMIC	BLEU, R-L, METEOR
Abela et al. [2022]	Chest X-ray	–	DenseNet	–	–	–	Template	–	MIMIC	BLEU, CE
Wu et al. [2022]	Chest X-ray	–	ResNet	ContrasL	–	–	LSTM	–	IU, MIMIC	BLEU, R-L, METEOR, C-D
Tanwani et al. [2022]	Chest X-ray, Ques	Resizing, Image transformations, Tokenizing	ResNeXt	AT-Class, ContrasL	BERT	Attention	Transformer	–	IU	BLEU

Continued on next page

Table A1 – continued from previous page

Paper	Input data	Data preparation	Feature Learning			Feature Fusion	Generation	Training Strategy	Dataset	Metrics
			I-Archi	I-Module	NI					
Chen et al. [2022]	Chest X-ray	Resizing, Tokenizing, ConAtoL, RemoNAT	ResNet+ Transformer	AT-EC MM	–	–	R2Gen	–	IU	BLEU, R-L, METEOR
Kong et al. [2022]	Chest X-ray	Resizing	Transformer	–	–	–	Retrieval	–	IU, MIMIC	BLEU, R-L, METEOR, CE
Wang et al. [2022e]	Chest X-ray	Tokenizing, ConAtoL, RemoNAT, FreFilter	Transformer	AT-Class, ContrasL	–	FeatO	Transformer	–	MIMIC	BLEU, R-L, METEOR, C-D
Du et al. [2022]	Chest X-ray	–	ResNet	AT-Class	–	–	H-LSTM	–	IU	BLEU, R-L, METEOR
Kaur and Mittal [2022b]	Chest X-ray	Resizing, Tokenizing, ConAtoL, RemoNAT, FreFilter	VGG	AT-Class	–	FeatO	H-LSTM	ReinL	IU	BLEU, R-L, C-D
Tanida et al. [2023]	Chest X-ray	Resizing, Data augmentation, Removing redundant whitespaces	ResNet+ Faster-RCNN	AT-DS	–	–	Transformer	–	MIMIC, ImaGeno	BLEU, R-L, METEOR, C-D, CE
Wang et al. [2023d]	Chest X-ray	Tokenizing	Transformer	AT	–	–	Transformer	–	IU, MIMIC	BLEU, R-L, METEOR, C-D, CE
Li et al. [2023b]	Chest X-ray, Chest CT	Resizing, Tokenizing, FreFilter	DenseNet	AT-Graph	–	Attention	Transformer	–	IU, COV	BLEU, R-L, C-D, Com
Wu et al. [2023]	Chest X-ray	Tokenizing, ConAtoL, Removing irrelevant elements, FreFilter	ResNet+ Transformer	–	–	–	Transformer	ReinL, AT	IU, MIMIC	BLEU, R-L, METEOR
Li et al. [2023a]	Chest X-ray, KnowB, RealR	Tokenizing	Transformer	AT-Class, ContrasL	ECI, BERT	Attention	Transformer	–	IU, MIMIC	BLEU, R-L, METEOR, C-D, CE
Huang et al. [2023]	Chest X-ray, KnowB	Tokenizing, ConAtoL, RemoNAT, FreFilter	ResNet+ Transformer	–	ECI, BERT	FeatO, Attention	Transformer	–	IU, MIMIC	BLEU, R-L, METEOR, CE
Zhang et al. [2023b]	Chest X-ray	–	DenseNet+ Transformer	AT-Graph, AT-Class, AT-EC	–	–	Transformer	AT	IU, MIMIC	BLEU, R-L, METEOR, CE
Xu et al. [2023]	Chest X-ray, Dermoscopy, KnowB	–	DenseNet+ Transformer	AT-Class	ECI, BERT	Attention	R2Gen	–	IU	BLEU, R-L, METEOR, Com

Continued on next page

Table A1 – continued from previous page

Paper	Input data	Data preparation	Feature Learning			Feature Fusion	Generation	Training Strategy	Dataset	Metrics
			I-Archi	I-Module	NI					
Yang et al. [2023]	Chest X-ray, KnowB	Resizing, Tokenizing, ConAtoL, FreFilter	ResNet	AT-Class, AT-EC	–	Attention	Transformer	–	IU, MIMIC	BLEU, C-D, CE
Zhang et al. [2023a]	Chest X-ray, Chest CT	Resizing	ResNet+ Transformer	–	–	–	Transformer+ MM	–	IU, MIMIC, COV	BLEU, R-L, METEOR
Wang et al. [2023a]	Chest X-ray	–	ResNet+ Transformer	AT-Class, AT-DS	–	–	R2Gen +LLM	–	MIMIC	CE
Lin et al. [2023]	Chest X-ray, Retil	Resizing, Tokenizing, FreFilter	ResNet+ Transformer	ContrasL	–	–	Transformer	–	IU, MIMIC, Ret-I, Ret-C	BLEU, R-L, METEOR
Selivanov et al. [2023]	Chest X-ray	Resizing, Tokenizing, ConAtoL, RemoNAT	DenseNet	–	–	–	Transformer	–	IU, MIMIC	BLEU, R-L, C-D, CE
Cao et al. [2023]	Chest X-ray, GEI, Term	–	DenseNet+ Transformer	–	BERT	FeatO, Attention, MM	Transformer	–	IU, MIMIC	BLEU, R-L, METEOR, C-D
Shetty et al. [2023]	Chest X-ray	–	Self-design	–	–	–	LSTM	–	IU	BLEU
Wang et al. [2023c]	Chest X-ray	–	ResNet+ Faster-RCNN+ Transformer	–	–	–	R2Gen	–	IU, MIMIC, ImaGeno	BLEU, R-L, METEOR
Li et al. [2023d]	Chest X-ray	Resizing, Cropping, Tokenizing, FreFilter, ConAtoL, RemoNAT	Transformer	–	–	MM +Self-design	Transformer	AT	IU, MIMIC	BLEU, R-L, METEOR, C-D
Liu et al. [2023b]	Chest X-ray, Term, RealR	FreFilter, ConAtoL	DenseNet	ContrasL	Transformer	FeatO, Attention	Transformer	–	IU, MIMIC	BLEU, R-L, METEOR
Wang et al. [2023b]	Chest X-ray	–	ResNet+ Transformer	ContrasL	–	–	R2Gen	–	IU, MIMIC	BLEU, R-L, METEOR, C-D
Pellegrini et al. [2023]	Chest X-ray, Ques	–	EfficientNet	–	BERT	Attention	Classification	–	Rad-ReStruct	CE
Dalla Serra et al. [2023a]	Chest X-ray, ClinicalI	Resizing, Cropping, Grouping	ResNet+ Faster-RCNN	AT-DS	Embedding layer	Attention	Transformer	–	MIMIC, ImaGeno	BLEU, R-L, METEOR, CE
Li et al. [2023c]	Chest X-ray, RealR, Term	Resizing, Self-design	ResNet+ Transformer	–	ECI, BERT	Attention	Transformer	–	IU, MIMIC	BLEU, R-L, METEOR, C-D
Dalla Serra et al. [2023b]	Chest X-ray, ClinicalI	Resizing, Cropping	ResNet+ Faster-RCNN	AT-DS, AT-Graph	Embedding layer	Attention	Transformer	–	MIMIC, ImaGeno	BLEU, R-L, METEOR, CE
Jeong et al. [2024]	Chest X-ray	Resizing	Transformer	–	–	–	Retrieval	–	MIMIC	BLEU, Score

Continued on next page

Table A1 – continued from previous page

Paper	Input data	Data preparation	Feature Learning			Feature Fusion	Generation	Training Strategy	Dataset	Metrics
			I-Archi	I-Module	NI					
Gu et al. [2024]	Chest X-ray, Term	Resizing, Cropping, Flipping, FreFilter, RemoNAT	ResNet	AT-DS, AT	Transformer	FeatO, Attention	Transformer	ReinL	IU, MIMIC	BLEU, R-L, METEOR, CE
Wang et al. [2024b]	Chest X-ray, Chest CT	–	ResNet+ Transformer	AT	–	–	Transformer	ReLoss	IU, COV	BLEU, R-L, METEOR, Grading
Xue et al. [2024]	Chest X-ray, Term	-	ResNet+ Transformer	-	Transformer, Attention	FeatO, Attention	Transformer	-	IU, MIMIC	BLEU, R-L, METEOR
Wang et al. [2024a]	Chest X-ray	Resizing, Cropping	DenseNet+ Transformer	AT-Class	–	–	R2Gen	AT	IU, MIMIC	BLEU, R-L, METEOR, C-D, CE
Jin et al. [2024]	Chest X-ray, RealR	–	ResNet	AT-Class	Transformer	FeatO, Attention	Transformer	–	IU, MIMIC	BLEU, R-L, METEOR, CE

Table A2: Comparisons of the model performance on the MIMIC-CXR Dataset. B1, B2, B3, B4, R-L, C-D, P, R, and F represent BLEU-1, BLEU-2, BLEU-3, BLEU-4, ROUGE-L, CIDEr-D, precision, recall, and F1 score, respectively. **The best** and **second best** results are highlighted. All values were extracted from their papers.

Paper	B1↑	B2↑	B3↑	B4↑	R-L↑	METEOR↑	C-D↑	P↑	R↑	F↑
Findings Section										
Chen et al. [2021]	0.353	0.218	0.148	0.106	0.278	0.142	-	0.334	0.275	0.278
Pino et al. [2021]	-	-	-	-	0.185	-	0.238	0.381	0.531	0.428
Song et al. [2022]	0.360	0.227	0.156	0.117	0.287	0.148	-	0.444	0.297	0.356
Impression + Findings Section										
Wu et al. [2022]	0.340	0.212	0.145	0.103	0.270	0.139	0.109	-	-	-
Wang et al. [2022d]	0.351	0.223	0.157	0.118	0.287	-	0.281	-	-	-
Jia et al. [2022]	0.363	0.228	0.156	0.130	0.300	-	-	-	-	-
Unspecified generated sections										
Liu et al. [2021a]	0.344	0.217	0.140	0.097	0.218	0.133	-	-	-	-
Liu et al. [2021c]	0.350	0.219	0.152	0.109	0.283	0.151	-	0.352	0.298	0.303
Liu et al. [2021b]	0.360	0.224	0.149	0.106	0.284	0.149	-	-	-	-
Li et al. [2023c]	0.360	0.231	0.162	0.119	0.298	0.153	0.217	-	-	-
Lin et al. [2023]	0.362	0.227	0.155	0.113	0.283	0.142	-	-	-	-
Zhang et al. [2023b]	0.362	0.229	0.157	0.113	0.284	0.153	-	0.380	0.342	0.335
Yang et al. [2022]	0.363	0.228	0.156	0.115	0.284	-	0.203	0.458	0.348	0.371
Wang et al. [2023c]	0.363	0.235	0.164	0.118	0.301	0.136	-	-	-	-
Liu et al. [2021d]	0.369	0.231	0.156	0.118	0.295	0.153	-	0.389	0.362	0.355
Xue et al. [2024]	0.372	0.233	0.154	0.112	0.286	0.152	-	-	-	-
Wang et al. [2024a]	0.374	0.230	0.155	0.112	0.279	0.145	0.161	0.483	0.323	0.387
Zhang et al. [2023a]	0.376	0.233	0.157	0.113	0.276	0.144	-	-	-	-
You et al. [2021]	0.378	0.235	0.156	0.112	0.283	0.158	-	-	-	-
Qin and Song [2022]	0.381	0.232	0.155	0.109	0.287	0.151	-	0.342	0.294	0.292
Wu et al. [2023]	0.383	0.224	0.146	0.104	0.280	0.147	-	-	-	0.758
Yang et al. [2023]	0.386	0.237	0.157	0.111	0.274	-	0.111	0.420	0.339	0.352
Wang et al. [2023b]	-	-	-	0.119	0.286	0.158	0.259	-	-	-
Wang et al. [2023d]	0.386	0.250	0.169	0.124	0.291	0.152	0.362	0.364	0.309	0.311
Liu et al. [2023b]	0.391	0.249	0.172	0.125	0.304	0.160	-	-	-	-
Huang et al. [2023]	0.393	0.243	0.159	0.113	0.285	0.160	-	0.371	0.318	0.321
Wang et al. [2022b]	0.395	0.253	0.170	0.121	0.284	0.147	-	-	-	-
Jin et al. [2024]	0.398	-	-	0.112	0.268	0.157	-	0.501	0.509	0.476
Wang et al. [2022e]	0.413	0.266	0.186	0.136	0.298	0.170	0.429	-	-	-
Kong et al. [2022]	0.423	0.261	0.171	0.116	0.286	0.168	-	0.482	0.563	0.519